

A comprehensive phase diagram for logistic populations in fluctuating environment.

Yitzhak Yahalom and Nadav M. Shnerb

Department of Physics, Bar-Ilan University, Ramat-Gan IL52900, Israel.

Population dynamics reflects an underlying birth-death process, where the rates associated with different events may depend on external environmental conditions and on the population density. A whole family of simple and popular deterministic models (like logistic growth) support a transcritical bifurcation point between an extinction phase and an active phase. Here we provide a comprehensive analysis of the phases of that system, taking into account both the endogenous demographic noise (random birth and death events) and the effect of environmental stochasticity that causes variations in birth and death rates. There phases are identified: an inactive phase in which mean time to extinction T scales logarithmically with the initial population size, a temporal Griffiths phase where $T \sim N^q$, where N is the carrying capacity, and an exponential phase with $T \sim \exp(\alpha N)$. All three phases and the transitions between them are studied in detail. The breakdown of the continuum approximation is identified inside the Griffiths phase, and the accompanied changes in decline modes are analyzed. The applicability of the emerging picture to the analysis of ecological timeseries and to the management of conservation efforts is briefly discussed.

I. INTRODUCTION

All environments fluctuate. Temperature, precipitation, wind velocity, predation pressure and food availability vary on all relevant spatio-temporal scales, from microns to continents, from microseconds to ages. These fluctuations affect the reproductive success of individuals and this, in turn, yields abundance variations that govern community structure and the evolutionary process. Through this paper we consider the fate of a population in stochastic environment.

The effect of environmental variations on conspecific individuals may be classified according to the level of correlations. In one extreme we think about an accidental encounter with a predator or with a piece of food, events that affect individuals in an uncorrelated manner. In the other extreme, droughts or cold waves may affect coherently entire populations. In reality one should expect a whole spectrum of stochastic perturbations and disturbances that influence groups of variable size. Nevertheless, for the sake of simplicity the corresponding theory distinguishes between *demographic stochasticity* (aka drift, shot noise), i.e., those aspects of noise that influence individuals in a completely uncorrelated manner, and *temporal environmental stochasticity*, that acts on entire populations [1].

Demographic noise yields abundance fluctuations that scale with the square root of the population size, while environmental stochasticity leads to variations that scale linearly with the abundance. Accordingly, one should expect that environmental stochasticity is the dominant mechanism. A few recent large-scale empirical studies show that abundance fluctuations for populations with n individuals indeed scale linearly with n [2–5]. On the other hand, demographic stochasticity provides the only scale against which the intensity of environmental variations may be measured [6–8]. Moreover, since demographic noise controls the low-density states of the system, it dictates important quantities like extinction times and species richness [9]. Consequently, the study of models that combine deterministic effects, temporal environmental stochasticity and demographic noise, received a considerable attention during the last years [6, 7, 10–16].

Here we would like to consider, within this framework, the simplest and the most important model of population dynamics, in which the abundance n satisfies a logistic, or logistic like, process. Some of our main findings were presented in brief in a recent work [17]; in this paper we provide the full analysis and discuss in detail the various transitions in that system and the implications of our work to the theory of population and community dynamics.

The logistic equation,

$$\frac{dn}{dt} = r_0 n - \beta n^2, \quad (1)$$

describes a very simple process that involves exponential (Malthusian) growth and negative density response (usually due to resource depletion). r_0 corresponds to the low-density growth rate of the population. As n increases, the growth decreases until the population saturates at $n^* = r_0/\beta$.

Technically speaking, the deterministic dynamics of Eq. (1) supports a transcritical bifurcation. When r_0 is positive the fixed point at $n = 0$ is unstable and n^* is a stable fixed point. If $r_0 < 0$ the only stable and feasible fixed point is the extinction state $n = 0$. At the transition, $r_0 = 0$, the population decays asymptotically like $1/t$, as opposed to the exponential decay below the transition. A wide variety of models support a transcritical bifurcation. These include the θ -logistic equation (where $\dot{n} = r_0 n[1 - (n/K)^\theta]$, The logistic system corresponds to $\theta = 1$), ceiling models (growth rate is kept fixed but the population cannot grow above a given carrying capacity, corresponds to $\theta = \infty$),

Ricker dynamics and so on. For the sake of concreteness, in what follows we will analyze a specific model. However, in section XI we will show that the outcomes of our study hold for all the systems that belong to the transcritical bifurcation class.

Since the actual number of individuals in a population is always an integer, Eq. (1) and its variants can only be understood as the deterministic limit of an underlying stochastic process, in which birth ($A \rightarrow 2A$), death ($A \rightarrow \emptyset$) or competition (say, $A + A \rightarrow A$) occur at random. For demographic noise of that kind the empty state $n = 0$ is the only absorbing state, so each population, for any set of parameters, must reach extinction in the long run. Under pure demographic stochasticity, when each individual is affected independently by the environmental fluctuations, the sign of r_0 determines the mean time to extinction T . When $r_0 < 0$, T is logarithmic in the initial population size n and does not depend on the carrying capacity. For $r_0 > 0$ the mean time T grows exponentially with n^* . At the bifurcation transition point ($r_0 = 0$) the functional form of the time to extinction depends on the initial condition n as we shall see below (section VII).

Another aspect of the transition between the logarithmic and the exponential behavior has to do with the applicability of the corresponding continuum (Fokker-Planck or backward Kolmogorov) equations. These differential equations emerge from the underlying difference (master) equation of the stochastic process via the continuum approximation, which fails when the relevant function (e.g., the mean time to extinction given n , $T(n)$) is not smooth enough over the integers. The continuum approximation fails in the exponential phase, and gives wrong estimations for the lifetime of the system. To overcome this difficulty, a WKB technique has been proposed by Kessler and Shnerb [18], and we will implement a similar approach in the relevant cases hereon.

The aim of this paper is to provide a comprehensive analysis of a logistic system that supports a finite number, N , of individuals (n^* is proportional to N) under the influence of both demographic and environmental stochasticity. This problem was considered by a few authors [1, 19–21] for the case where the strength of environmental fluctuations is *unbounded*, for example when the amplitude of these variations is an Ornstein-Uhlenbeck process. In that case there are always (very rare) periods in which the net growth rate is negative, and (as we shall see below) these periods dominate the large N asymptotic behavior of the extinction times. As a result, the system admits only two phases: an inactive (logarithmic) phase and a temporal Griffiths phases [22] where T scales with N like a power-law.

We consider a system under dichotomous (telegraphic) noise, with finite amplitude σ and correlation time τ . Since the noise is bounded, above a certain value of r_0 the growth rate is always positive, so the system allows for another transition, between the temporal Griffiths phase and the exponential phase. We provide a unified analysis of all the three phases and the phase transitions between them.

Inside the Griffith phase we identify three (perhaps related) transitions, or crossovers: the failure of the continuum approximation, the opening of a spectral gap for the corresponding Markov matrix and a qualitative shift between soft and sharp decline modes. In what follows we shall discuss these transitions and their relevance to the analysis of empirical datasets.

In the next section a generic phase diagram for transcritical systems with bounded environmental stochasticity is presented and discussed. The reader is referred, from each part of the diagram, to the relevant section.

II. THE PHASE DIAGRAM

This paper is organized around the phase diagram shown in Figure 1. The x -axis of figure 1 is the time averaged value of the linear growth rate, r_0 , and the y axis corresponds to σ , the amplitude of environmental variations. Demographic noise affect the system in any case.

Three phases are identified:

- **Extinction (logarithmic) phase:** In the red region, $r_0 < 0$, the time average of the linear growth rate is negative. In this regime the time to extinction grows *logarithmically* with the *initial population size*, $T \sim \ln n$. The overall capacity of the system, N , only limits the maximum value of n at $t = 0$ so it sets the scale for the maximum lifetime, but for fixed $n(t = 0)$, the mean lifetime T is independent of N .

In this logarithmic regime one may analyze the corresponding stochastic process by taking the continuum limit of the backward Kolmogorov equation, as explained in section IV. Results for this regime are presented in Section V.

- **Temporal Griffiths (power-law) phase:** In the green region where $0 < r_0 < \sigma$, the mean growth rate is positive but the instantaneous growth rate may become negative because of the environmental variations. Below (sections V and VIII) we consider this regime and show that the time to extinction grows like a power-law in N . Here the large- N -dependence of T is not affected by the initial conditions and the difference between T for a single individual and for N individuals appears only in the prefactor. Put it another way, the chance of establishment for a single individual is N independent.

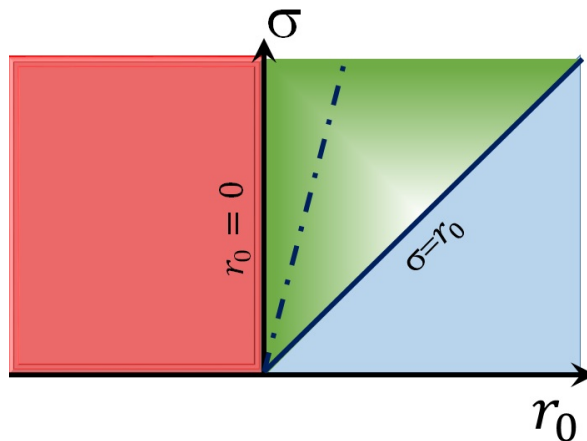


FIG. 1: A phase diagram for a logistic system under demographic and bounded environmental stochasticity, presented in the r_0 - σ plane. In the inactive phase ($r_0 < 0$, red) the time to extinction scales like $\ln n(t=0)$ where N plays no role, except of setting an upper bound for $n(t=0)$. In the exponential phase $r_0 > \sigma$ (blue) the extinction time grows exponentially with N . When $\sigma > 0$ the logarithmic and the exponential phases are separated by a finite power-law region (temporal Griffiths phase, green). At the logarithmic-power transition ($r_0 = 0$, $\sigma > 0$) T grows like $\ln^2 N$, while at the Griffiths-exponential transition T is a stretched exponential in N . The dashed-dotted line indicates the failure of the continuum (diffusive) approximation, which is correlated with the transition between soft and sharp decline mode.

- **Active (exponential) phase:** In the blue region $r_0 > \sigma$, the linear growth rate is always positive. In this regime the mean time to extinction grows exponentially with N , $T \sim \exp(\alpha N)$. In section IX we show that α is related to the dynamics of a system with time-independent growth rate $r_0 - \sigma$, while growth rate variations contribute only to the power-law pre-factor of this exponent.

Three types of transition regions between these phases are discussed below:

- When there are no environmental variations ($\sigma = 0$), the transition point at the origin of the x -axis separates the logarithmic (N -independent) and the exponential phase. This point is analyzed in section VII. At the transition point the scaling of T with N depend on the initial conditions, and ranges between $T \sim \ln N$ for a single individual to $T \sim \sqrt{N}$ when the initial state is a finite fraction of N (Eq. 49).
- The y axis of Fig. 1, where $r_0 = 0$ but $\sigma > 0$, marks the transition between the logarithmic and the power-law Griffiths phase when the environment fluctuates. Again, along this line the N scaling of the time to extinction depends on the initial conditions, but now it runs between $\ln N$ for a single individual to $\ln^2 N$ for finite fraction.
- The line $\sigma = r_0$ marks the transition between the power-law and the exponential phase. This transition line is characterized by a stretched exponential scaling and is discussed in Section IX.

The phase diagram is based on the features of the mean time to extinction T . In section X we present some considerations and results for a more general quantity, the probability distribution function for exit times, $f(t) dt$.

As mentioned above, the continuum approximation breaks down inside the temporal Griffiths phase, and this is indicated by the **dashed-dotted line** in Fig. 1. In section VIII we present a WKB analysis which is valid even where the continuum approximation breaks and converges to the continuum result when r_0 is much smaller than σ . The power-law exponent predicted by this WKB analysis diverges when $\sigma \rightarrow r_0$, marking the transition to the third, exponential regime.

Another transitions that appears inside the temporal Griffiths phase, and are probably related to the breakdown of the continuum approximation, are the emergence of a spectral gap for the corresponding Markov matrix, the crossover between soft and sharp decline modes and the qualitative alteration of the quasi-stationary probability distribution function, these phenomena are discussed in Sections VIII and X.

In the next sections we present and analyzed a specific microscopic model but, as mentioned above, we believe that the general picture emerges - the phases, the different functional dependencies of T on N , and the characteristics of the transitions - are generic and will characterize any system that supports a transcritical bifurcation under demographic noise and bounded environmental stochasticity. In Section XI we implement our WKB analysis to support this argument.

Finally, the emerging insights and their relevance to the theoretical understanding and to the empirical analysis of many practical problems, ranging from the assessment of population viability and the management of conservation efforts to the general theory of species coexistence. A preliminary discussion of these points is presented in Section XII.

III. THE MODEL

The logistic equation (1) is the deterministic limit of many underlying stochastic processes. We would like to compare our analytic results with the numerical solutions of the corresponding Markov process, thus we prefer a process in which the total number of individuals is bounded. To that aim, we use a genetic model for two-allele (species) competition with one sided mutation, as defined in [23]. In section XI below we explain why the qualitative characteristics of the phase space diagram do not depend on the microscopic features of the model.

Let us consider a system with N individuals, n of them belong to species A and $N - n$ to species B. At each elementary step two individuals are drawn at random for a duel, the loser dies and the winner produces a single offspring. This is a zero sum model so N is kept fixed and there is only one degree of freedom, n . The endogenous demographic stochasticity is related to the discrete nature of the state variable n .

In case of an intraspecific competition (if two A-s or two B-s were chosen) both individuals have the same relative fitness and each of them wins with probability $1/2$. When interspecific duel takes place the chance of the A individual to win is

$$P_A = \frac{1}{2} + \frac{s(t)}{4}, \quad (2)$$

where the dependence of s on time reflects the effect of environmental fluctuations.

The outcome of each elementary duel is birth and death: the loser dies, and the winner produces a single offspring. When an A individual wins a duel, the offspring is also an A with probability $1 - \nu$, and with probability ν the offspring is a B-individual. One may consider that as a mutation from A to B. On the other hand, when a B wins a duel the offspring is always B, so the mutation is one-sided [23]. The possible outcomes of all kinds of duels are (note that the expressions above the arrows are probabilities, not rates),

$$\begin{array}{lll} B + B \xrightarrow{1} 2B & A + A \xrightarrow{1-\nu} 2A & A + A \xrightarrow{\nu} A + B \\ A + B \xrightarrow{1-P_A} 2B & A + B \xrightarrow{P_A(1-\nu)} 2A & A + B \xrightarrow{\nu P_A} A + B. \end{array} \quad (3)$$

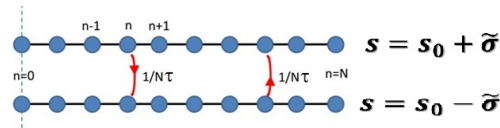


FIG. 2: A sketch of the possible states of two-allele competition with one sided mutation with demographic and environmental stochasticity. The abundance of the focal species is n , and in each elementary duel it may change to either $n + 1$ or $n - 1$. Under dichotomous noise $s = s_0 + \tilde{\sigma}$ (upper channel) or $s = s_0 - \tilde{\sigma}$ (lower channel). The chance of environmental flip is $1/N\tau$ per elementary step, so the persistence time of the environment is τ generations, where a generation is N elementary duels. The state $n = 0$ is absorbing, while the system may escape from the state $n = N$ due to mutations.

To specify the stochastic process completely we have to define the dynamics of $s(t)$. We define $s(t) = s_0 + \eta(t)$, where s_0 is the mean (logarithmic) relative fitness of species A and $\eta(t)$ is a zero-mean stochastic process. As we shall see, in many cases the only important characteristics of this process are its correlation time τ and its amplitude σ .

We consider a system with dichotomous (telegraphic) environmental noise, so $\eta = \pm\tilde{\sigma}$. After each elementary step η may switch (from $\pm\tilde{\sigma}$ to $\mp\tilde{\sigma}$, see Fig. 2) with probability $1/N\tau$, so the persistence time of the environment is taken from a geometric distribution with mean $N\tau$ steps, or (if time is measured in units of generation, N duels correspond to a single generation) τ generations. Dichotomous noise of this kind may imitate the features of other generic distributions, like Gaussian or Poisson noise, see Appendix B. However, dichotomous noise is bounded, and this makes a difference in some circumstances, as explained in section VIII.

The chance of an interspecific duel for two, randomly picked individuals is

$$F_n = 2n(N - n)/N(N - 1),$$

and the chance for an A-intraspecific duel is

$$Q_n = n(n-1)/N(N-1).$$

If

$$P_A^+ = 1/2 + s_0/4 + \tilde{\sigma}/4$$

stand for the chance of an A individual to win against a B in the $+\sigma$ state, and

$$P_A^- = 1/2 + s_0/4 - \tilde{\sigma}/4$$

is the chance to win in the minus state, the transition probabilities are:

$$\begin{aligned} W_{n \rightarrow n-1}^{++} &= \left(1 - \frac{1}{\tau N}\right) [F_n(1 - P_A^+) + \nu Q_n] & W_{n \rightarrow n+1}^{++} &= \left(1 - \frac{1}{\tau N}\right) [(1 - \nu)F_n P_A^+] \\ W_{n \rightarrow n-1}^{--} &= \left(1 - \frac{1}{\tau N}\right) [F_n(1 - P_A^-) + \nu Q_n] & W_{n \rightarrow n+1}^{--} &= \left(1 - \frac{1}{\tau N}\right) [(1 - \nu)F_n P_A^-] \\ W_{n \rightarrow n-1}^{-+} &= \frac{1}{\tau N} [F_n(1 - P_A^+) + \nu Q_n] & W_{n \rightarrow n+1}^{-+} &= \frac{1}{\tau N} [(1 - \nu)F_n P_A^+] \\ W_{n \rightarrow n-1}^{+-} &= \frac{1}{\tau N} [F_n(1 - P_A^-) + \nu Q_n] & W_{n \rightarrow n+1}^{+-} &= \frac{1}{\tau N} [(1 - \nu)F_n P_A^-]. \end{aligned} \quad (4)$$

The mean time to extinction for species A when it is represented by n individuals in the plus state, T_n^+ , and the corresponding quantity in the minus state, T_n^- , satisfy the discrete backward Kolmogorov equation (BKE),

$$\begin{aligned} T_n^+ &= W_{n \rightarrow n+1}^{++} T_{n+1}^+ + W_{n \rightarrow n-1}^{++} T_{n-1}^+ + (1 - W_{n \rightarrow n+1}^{++} - W_{n \rightarrow n-1}^{++}) T_n^+ \\ &\quad + W_{n \rightarrow n+1}^{+-} T_{n+1}^- + W_{n \rightarrow n-1}^{+-} T_{n-1}^- + (1 - W_{n \rightarrow n+1}^{+-} - W_{n \rightarrow n-1}^{+-}) T_n^- + \frac{1}{N} \\ T_n^- &= W_{n \rightarrow n+1}^{--} T_{n+1}^- + W_{n \rightarrow n-1}^{--} T_{n-1}^- + (1 - W_{n \rightarrow n+1}^{--} - W_{n \rightarrow n-1}^{--}) T_n^- \\ &\quad + W_{n \rightarrow n+1}^{-+} T_{n+1}^+ + W_{n \rightarrow n-1}^{-+} T_{n-1}^+ + (1 - W_{n \rightarrow n+1}^{-+} - W_{n \rightarrow n-1}^{-+}) T_n^+ + \frac{1}{N}. \end{aligned} \quad (5)$$

The boundary conditions at the absorbing state are $T_0^+ = T_0^- = 0$. In the other end $n = N$ the boundary conditions are determined by the relationships (imposed by the transition probabilities) between T_{N-1}^\pm and T_N^\pm (see below).

The linear equation (5), with the appropriate definitions for the W s, may be solved numerically by matrix inversion or using a transfer matrix technique, as explained in detail in Appendix A. In what follows we compare our analytic results with the outcomes of these numerical calculations, where the use of algorithms for sparse matrices and quadruple precision allows us to consider systems up to $N = 10^7$.

In analogy to Eq. (1), the deterministic dynamics of n in our model is given by

$$\dot{n} = r(t)n - \beta(t)n^2, \quad (6)$$

where

$$r(t) \equiv s_{eff} \pm \sigma - \nu,$$

$$\beta(t) = N(s_{eff} \pm \sigma).$$

Here $s_{eff} \equiv s_0(1 - \nu/2)$ and $\sigma \equiv \tilde{\sigma}(1 - \nu/2)$. The \pm correspond to the plus and the minus state.

IV. THE CONTINUUM APPROXIMATION

Using a linear transformation,

$$T_n \equiv (T_n^+ + T_n^-)/2 \quad \Delta_n \equiv (T_n^+ - T_n^-)/2,$$

one may rewrite (5) in a more informative manner, since T_n is the mean time to extinction where the average is taken over both histories and initial state of the environment. In the limit $N \gg 1$ the continuum approximation is used.

n/N is replaced by x , $n \pm 1 \equiv x \pm 1/N$, and all the functions T and W are expanded to second order in $1/N$. The resulting set of equations is,

$$\begin{aligned} \left(s_0(1 - \nu/2) - \frac{\nu}{1-x}\right) T'(x) + \left(1 + \frac{\nu}{2} \left[\frac{2x-1}{1-x} - \frac{s_0}{2}\right]\right) \frac{T''(x)}{N} + \tilde{\sigma}(1 - \nu/2) \Delta'(x) - \frac{\tilde{\sigma}\nu\Delta''(x)}{4N} &= -\frac{1}{x(1-x)} \\ \left(s_0(1 - \nu/2) - \frac{\nu}{1-x}\right) \Delta'(x) + \left(1 + \frac{\nu}{2} \left[\frac{2x-1}{1-x} - \frac{s_0}{2}\right]\right) \frac{\Delta''(x)}{N} + \tilde{\sigma}(1 - \nu/2) T'(x) - \frac{\tilde{\sigma}\nu T''(x)}{4N} &= \frac{2N}{N\tau - 2} \frac{\Delta}{x(1-x)}. \end{aligned} \quad (7)$$

Below (section VIII) we will discuss possible failures of the continuum approximation and will explain how to overcome these difficulties, but in the next few sections we assume the validity of Eqs. (7) and review the outcomes.

To proceed, we make the following steps,

1. We assume $N\tau \gg 1$, so $N\tau - 2 \approx N\tau$. This implies that as N is taken to be large τ is kept finite, i.e., that the persistence time of the environment is independent of the size of the community.
2. In the second Equation of (7) only the Δ and the T' terms are kept. In general, applying a dominant balance argument one finds two dominant terms in the large N limit. One of them must be the Δ term, otherwise the result is independent of the persistence time of the environment τ , which is physically impossible. This term must be balanced by one of the T terms (if this is not the case $\Delta = 0$ is a solution and environmental stochasticity has no effect), and the continuum approximation is valid only if $T' \gg T''/N$. Using that we can solve for Δ and plug the solution into the upper equation of (7).
3. The Δ'' term in the upper equation is neglected, again this holds when the continuum approximation is applicable.

Under these approximations, Eqs (7) reduce to a single, second order, inhomogeneous differential equation for T ,

$$\begin{aligned} \left(s_0(1 - \nu/2) - \frac{\nu}{1-x} + \frac{[\tilde{\sigma}(1 - \nu/2)]^2\tau}{2}(1 - 2x)\right) T'(x) + \\ \left(1 + \frac{\nu}{2} \left[\frac{2x-1}{1-x} - \frac{s_0}{2}\right] + \frac{N[\tilde{\sigma}(1 - \nu/2)]^2\tau}{2}x(1-x)\right) \frac{T''(x)}{N} &= -\frac{1}{x(1-x)}. \end{aligned} \quad (8)$$

Now one likes to define

$$g \equiv \sigma^2\tau/2. \quad (9)$$

Under pure environmental stochasticity the growth/decay of $\ln x_0$ during τ is $\ln x_0 \rightarrow \ln x_0 \pm \sigma\tau$, so g is the diffusion constant of the system along the logarithmic abundance axis.

Assuming further $\nu \ll 1$ and $s_0 \ll 1$ (this implies that the deterministic growth/decay during one generation is small with respect to the population size), Eq. (8) takes the form,

$$\left(s_{eff} - \frac{\nu}{1-x} + g(1 - 2x)\right) T'(x) + \left(\frac{1}{N} + gx(1-x)\right) T''(x) = -\frac{1}{x(1-x)}. \quad (10)$$

In the next sections we will analyze this equation. As we shall see, the qualitative characteristics of T depends on the value of the (time averaged) low density reproduction rate,

$$r_0 \equiv s_{eff} - \nu. \quad (11)$$

The boundary conditions for Eq. (10) are derived from the discrete equations in the appropriate limit. Since $T^+(0) = T^-(0) = 0$, in the continuum limit $T(0) = 0$. In the reflecting boundary $x = 1$ one may use the discrete equations

$$\begin{aligned} T_N^+ &= (1 - 1/N\tau)[(1 - \nu)T_N^+ + \nu T_{N-1}^+] + (1/N\tau)[(1 - \nu)T_N^- + \nu T_{N-1}^-] + 1/N \\ T_N^- &= (1 - 1/N\tau)[(1 - \nu)T_N^- + \nu T_{N-1}^-] + (1/N\tau)[(1 - \nu)T_N^+ + \nu T_{N-1}^+] + 1/N \end{aligned} \quad (12)$$

so

$$T_N = (T_N^+ + T_N^-)/2 = (1 - \nu)T_N + \nu T_{N-1} + 1/N. \quad (13)$$

Accordingly,

$$T'(1) = \frac{1}{\nu}.$$

V. MEAN TIME TO EXTINCTION: AN ASYMPTOTIC MATCHING APPROACH

To find the large N behavior of the lifetime $T(x)$ we would like to solve Eq. (10) in different regimes, then we will use an asymptotic matching techniques to determine the constants of integration.

In the *inner regime* $x \ll 1$ so $1 - x \sim 1$. Accordingly, (10) takes the form

$$[(1 + Gx)T'_{in}]' + r_0 N T'_{in} = \frac{-N}{x}, \quad (14)$$

with $G \equiv Ng$ and the relevant boundary condition is $T(0) = 0$. One integration is thus trivial, and using an integrating factor one obtains,

$$T_{in}(x) = \frac{c_1}{Nr_0} \left(1 - \frac{1}{(1 + Gx)^{r_0/g}} \right) - \frac{N}{(1 + Gx)^{r_0/g}} I(x), \quad (15)$$

where,

$$I(x) \equiv \int_0^x \frac{\ln t \, dt}{(1 + Gt)^{1-r_0/g}}. \quad (16)$$

In the *outer regime* $x \gg 1/G$, the demographic stochasticity term $1/N$ in Eq. (10) is negligible. This yields,

$$[gx(1 - x)]T''_{out}(x) + \left(s_{eff} + g(1 - 2x) - \frac{\nu}{1 - x} \right) T'_{out} = \frac{-1}{x(1 - x)}, \quad (17)$$

or,

$$Q'(x) + \left(\frac{s_{eff}/g}{x(1 - x)} - \frac{\nu/g}{x(1 - x)^2} \right) Q(x) = \frac{-1}{x(1 - x)}, \quad (18)$$

with $Q \equiv gx(1 - x)T'_{out}$. Using an integrating factor,

$$\left(Q(x) \left(\frac{x}{1 - x} \right)^{r_0/g} e^{-\frac{\nu/g}{1-x}} \right)' = - \left(\frac{x^{-1+r_0/g}}{(1 - x)^{1+r_0/g}} \right) e^{-\frac{\nu/g}{1-x}}. \quad (19)$$

we obtained,

$$T'_{out}(x) = \frac{(1 - x)^{-1+r_0/g}}{gx^{1+r_0/g}} e^{\frac{\nu/g}{1-x}} \int_x^1 dt \frac{t^{-1+r_0/g}}{(1 - t)^{1+r_0/g}} e^{-\frac{\nu/g}{1-t}}. \quad (20)$$

This solution satisfies the required outer boundary condition $T'_{out}(1) = 1/\nu$. Defining $q \equiv (\nu t)/g(1 - t)$ one may solve the integral,

$$\int_x^1 dt \frac{t^{-1+r_0/g}}{(1 - t)^{1+r_0/g}} e^{-\frac{\nu/g}{1-t}} = \left(\frac{g}{\nu} \right)^{r_0/g} e^{-\nu/g} \int_{\frac{\nu x}{g(1-x)}}^{\infty} dq e^{-q} q^{-1+r_0/g} = \left(\frac{g}{\nu} \right)^{r_0/g} e^{-\nu/g} \Gamma \left(r_0/g, \frac{\nu x}{g(1-x)} \right), \quad (21)$$

where $\Gamma(a, x)$ is the incomplete Gamma function. Accordingly,

$$T'_{out}(x) = \frac{(1 - x)^{-1+r_0/g}}{gx^{1+r_0/g}} e^{\frac{x\nu}{g(1-x)}} \left(\frac{g}{\nu} \right)^{r_0/g} \Gamma \left(r_0/g, \frac{\nu x}{g(1-x)} \right). \quad (22)$$

Large argument asymptotics of the incomplete Gamma function shows that $T'(x) \approx 1/(\nu x^2)$ as $x \rightarrow 1$, as expected.

To find c_1 we matched the two solutions, T'_{in} and T'_{out} , when $1/G \ll x \ll 1$. In the limit $Gx \gg 1$ Eq. (15) yields,

$$T_{in}(Gx \gg 1) \sim \frac{c_1}{r_0 N} \left(1 - \frac{1}{(Gx)^{r_0/g}} \right) + \frac{g}{r_0^2} \left(1 - \frac{1}{x^{r_0/g}} \right) - \frac{\ln x}{r_0} - \frac{N}{(Gx)^{r_0/g}} I(1), \quad (23)$$

and,

$$T'_{in}(Gx \gg 1) \sim \left(\frac{c_1}{G^{r_0/g+1}} + \frac{1}{r_0} + \frac{r_0 I(1)}{g^2 G^{r_0/g-1}} \right) \frac{1}{x^{r_0/g+1}} - \frac{1}{r_0 x}, \quad (24)$$

with the $I(x)$ defined above (16).

Comparing Eq. (24) with the small x asymptotic of (20) one finds,

$$c_1 = G^{r_0/g+1} \frac{\Gamma(r_0/g)}{g} \left(\frac{g}{\nu}\right)^{r_0/g} - \frac{G^{r_0/g+1}}{r_0} - \frac{G^2 r_0 I(1)}{g^2}. \quad (25)$$

Note that $I(1)$ is a hypergeometric function, one can take gN to infinity and approximate

$$I(1) \approx -\frac{g^2}{r_0^2} (G)^{r_0/g-1} + \frac{\gamma_E + \ln G + \Psi(-r_0/g)}{Nr_0},$$

where Ψ is the digamma function.

A. Time to extinction for a single invader/mutant

Here we assume that $n(t=0) = 1$, or $x(t=0) = 1/N$. This corresponds to the case where a homogenous B population is invaded by a single A , or when (due to extremely rare mutations that never happens again) B mutates into A .

Since $I(1) - I(x)$ appears as the difference between two Beta functions, by taking first $x \rightarrow 0$ and then $G \rightarrow \infty$,

$$I(1) - I(x) \approx \frac{g}{Nr_0^2} \left((Gx)^{r_0/g} + r_0 x^{r_0/g} [\gamma_E + Nr_0 x + \ln Gx + \Psi(-r_0/g)] \right) - \frac{(1+Gx)^{r_0/g} \ln x}{Nr_0}. \quad (26)$$

Plugging (25) into (15), the mean lifetime of a single mutant $x = 1/N$ turns out to be

$$T(1/N) = \left(\frac{\Gamma(r_0/g) G^{r_0/g}}{r_0} \left(\frac{g}{\nu}\right)^{r_0/g} - \frac{\gamma_E + \ln(g) + \psi(-r_0/g)}{r_0} \right) \left(1 - (1+g)^{-r_0/g} \right) + (1+g)^{-r_0/g}. \quad (27)$$

When $r_0 > 0$ the mean persistence time is dominated by the first term of (27) and increases like $(Ng)^{r_0/g}$. This behavior is demonstrated in panel (A) of Fig. 3. When $r_0 < 0$ the time to extinction becomes N -independent in the large- N limit.

B. Time to extinction for macroscopic populations

For population of abundance n , if $ng \gg 1$ (or equivalently $Gx \gg 1$) the effect of demographic noise is weak. This condition allows one to approximate $I(1) - I(x)$ by neglecting 1 with respect to Gx . Plugging the outcome into the equation in the matching regime $x \ll 1$ one gets,

$$T_{in} = \left(G^{r_0/g} - x^{-r_0/g} \right) \frac{\Gamma(r_0/g)}{r_0} \left(\frac{g}{\nu}\right)^{r_0/g} - \frac{\ln Gx}{r_0} - \frac{\gamma_E - g/r_0 + \Psi(-r_0/g)}{r_0}. \quad (28)$$

Accordingly, the time to extinction grows, again, like $N^{r_0/g}$ if r_0 is positive [1, 19], as demonstrated in panel (B) of Figure 3. T is logarithmic in $n = Nx$ when r_0 is negative as depicted in panel (A) of Fig 4.

When x becomes larger, one would like to write down the time to extinction as

$$T(x) = \int_0^\xi T'_{in}(x) dx + \int_\xi^x T'_{out}(x) dx, \quad (29)$$

where ξ is somewhere in the overlap region $1/G \ll \xi \ll 1$. Since $T'_{out}(x)$ is N -independent, the only terms that diverge with N come from the first integral.

Note that, for $r_0 > 0$ the large N asymptotic of the mean lifetime of a single mutant (27) differs from the corresponding quantity for large population (28) only by the factor $1 - (1+g)^{-r_0/g}$, which converges to r_0 when $g \ll 1$. This factor represents the chance of establishment for a single beneficial mutant/immigrant. The probability of absorption at zero, for a random walker that moves to the right with probability $1/2 + r_0/4$ and to the left with probability $1/2 - r_0/4$, is given by $1 - r_0$ for $r_0 \ll 1$, so r_0 is the chance to escape the absorbing state. The time to extinction is N dependent only when the upper bound (the carrying capacity n^* , which is linear in N) determines the chance of extinction. For a single mutant the chance that the extinction happens because of this upper bound, and not as a result of the random walk in the log-abundance space, is equal to the chance of establishment $1 - (1+g)^{-r_0/g} \approx r_0$.

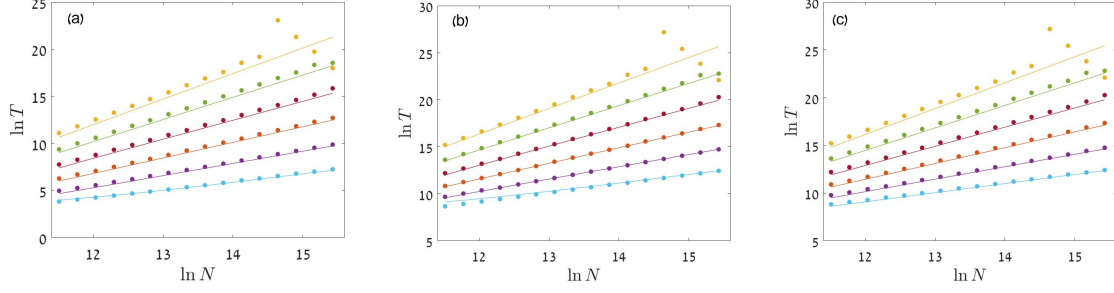


FIG. 3: The logarithm of T vs. $\ln N$ for $x(t=0) = 1/N$ (panel A), $x(t=0) = 0.01$ (panel B) and $x(t=0) = 1$ (panel C). Dots were obtained from numerical solution of the exact BKE (5), as explained in the methods section. The full lines are the prediction of Eq. 27 (panel A), Eq. 28 (panel B) and Eq. 31 (panel C). Parameters are $\tau = 2$, $\tilde{\sigma} = 0.08$, $s_0 = 0.1$. Different colors represent different mutation probabilities: $\nu = 0.088$ (light blue), 0.086 (purple), 0.084 (light red), 0.082 (red), 0.08 (green) and 0.078 (yellow). Once the population becomes macroscopic its time to extinction depends only weakly on its size, so the differences between panels (B) and (C) are only minor. At small ν and large N (yellow, upper right) our numeric becomes less accurate.

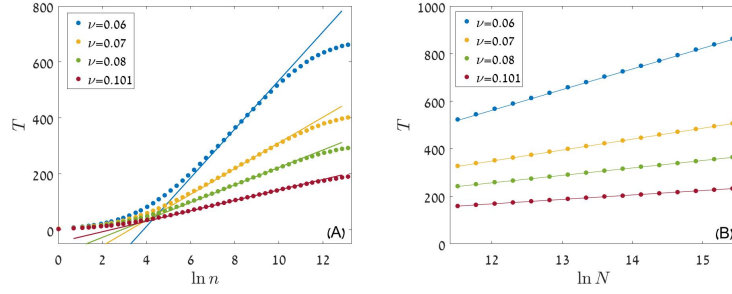


FIG. 4: In the left panel, the time to extinction is plotted against the initial log-abundance when $r_0 < 0$, i.e., in the inactive (logarithmic) phase. Parameters are $\tilde{\sigma} = 0.03$, $s_0 = 0.05$, $N = 500000$ and $\tau = 2$. As in Fig. 3, points are the numerical solution of the exact BKE while lines are analytic predictions. The lines represent the two last terms of Eq. (28). The theory fits the numerical experiment in the bulk, where the asymptotic matching works. Panel B (right) provides the results for $x(t=0) = 1$. The lines represent the predictions of Eq. (31) and the agreement is very good.

C. Time to extinction from maximal capacity

To calculate $T(1)$ one can compare $T(x) = T(1) + \int_1^x T'_{out}(t)dt$ in the matching regime ($1/G \ll x \ll 1$) with Eq. (28). Defining $q \equiv (\nu t)/g(1-t)$ we solve the integral and approximate the solution for $x \ll 1$

$$\frac{1}{g} \int_{\infty}^{(\nu x)/g(1-x)} e^q q^{-(1+r_0/g)} \Gamma(r_0/g, q) dq \approx \frac{\Psi(r_0/g) - \ln(\nu x/g)}{r_0} - \frac{\Gamma(r_0/g)}{r_0} \left(\frac{\nu x}{g} \right)^{r_0/g}. \quad (30)$$

a comparison between this result and Eq. (28) yields,

$$T(1) = \frac{\Gamma(r_0/g)}{r_0} \left(\frac{g}{r} \right)^{r_0/g} + \frac{2\Psi(-r_0/g) + \ln(\nu/Gg) - \gamma_E + g/r_0}{r_0}. \quad (31)$$

This result are demonstrated in panel (C) of Fig. 3 (for $r_0 > 0$) and in panel (B) of Fig. 4 for $r_0 < 0$.

VI. LIFETIME AT CRITICALITY

Through the last section we have assumed that in the power-law phase the term $G^{r_0/g}$ dominates, so one may neglect terms which are logarithmic in N , or $\mathcal{O}(1)$. This is the case for each $r_0 > 0$ as long as $N > n_c$ [12] where

$$n_c = \frac{e^{g/r_0} - 1}{g}. \quad (32)$$

n_c marks the point above which the deterministic grows, associated with r_0 , dominates both demographic and environmental fluctuations. As r_0 decreases while g is kept fixed, n_c grows exponentially and, for any fixed N , the system enters the regime where the deterministic growth term becomes negligible. This is the critical regime that separates the power-law and the N -independent phase, and here we discuss the mean time to extinction in this regime.

When the linear growth rate vanishes ($r_0 = 0$, $s_{eff} = -\nu$), Eq. (10) takes the form,

$$\left(-\frac{\nu x}{1-x} + g(1-2x)\right) T'(x) + \left(\frac{1}{N} + gx(1-x)\right) T''(x) = -\frac{1}{x(1-x)}. \quad (33)$$

In the outer regime the $1/N$ term is negligible and,

$$\left(-\frac{\nu x}{1-x} + g(1-2x)\right) T'(x) + gx(1-x) T''(x) = -\frac{1}{x(1-x)}. \quad (34)$$

The definition $Q = gx(1-x)T'_{out}$ allows one to write a first order equation for Q ,

$$Q' - \frac{\nu Q}{g(1-x)^2} = -\frac{1}{x(1-x)}, \quad (35)$$

and this equation may be solved for T' ,

$$T'_{out}(x) = c_2 \frac{e^{\nu/g(1-x)}}{x(1-x)} + \frac{e^{\nu x/g(1-x)}}{gx(1-x)} Ei\left(\frac{\nu x}{g(1-x)}\right). \quad (36)$$

To satisfy the right boundary condition $T'(1) = 1/\nu$, c_2 must vanish.

In the inner regime where $1-x \approx 1$ we can use the definition $G \equiv gN$ and $W = (1+Gx)T'_{in}$ to write,

$$\begin{aligned} W' - \frac{N\nu x}{1+Gx} W &= -\frac{N}{x} \\ \left(W e^{-\nu x/g} (1+Gx)^{\nu/g^2 N}\right)' &= -N \frac{e^{-\nu x/g} (1+Gx)^{\nu/g^2 N}}{x} \end{aligned} \quad (37)$$

As long as $\nu/g^2 \ll N/\ln N$ (that is, g is not vanishingly small), the term $(1+Gx)^{\nu/g^2 N}$ tends to one when N is large. Therefore,

$$T'_{in} = \frac{N e^{\nu x/g}}{1+Gx} [Ei(\nu x/g) - c_1], \quad (38)$$

and the matching between $T'_{in}(Gx \gg 1)$ and $T'_{out}(x \ll 1)$ dictates $c_1 = 0$.

Another integration, plus the boundary condition $T(x=0) = 0$, yields,

$$T_{in} \approx -\frac{1}{g} \left[\gamma_E + \log\left(\frac{\nu x}{g}\right) \right] \log(1+Gx) - \frac{Li_2(-Gx)}{g}, \quad (39)$$

where the dilogarithmic function $Li_2(-x) \sim \ln^2(x)$ when x approaches infinity. Accordingly, for a single mutant ($x = 1/N$) the only N dependence comes from the $\ln(\nu x/g)$ term and the time to extinction is logarithmic in N ,

$$T(1/N) \approx \frac{\ln(1+g)}{g} \ln N. \quad (40)$$

On the other hand, when $Gx \gg 1$ the $\ln^2 N$ behavior dominates [22]. For example, when $x \sim N^{-\beta}$ with $\beta < 1$, the argument of the dilogarithmic function approaches minus infinity with N and the leading contribution to the lifetime is,

$$T(x \sim N^{-\beta}) \sim \frac{(1-\beta^2)}{2g} \ln^2 N \quad (41)$$

As before, since T'_{out} is N -independent, the same $\ln^2 N$ behavior characterizes the outer regime. The validity of these formulas is demonstrated in Figure 5.

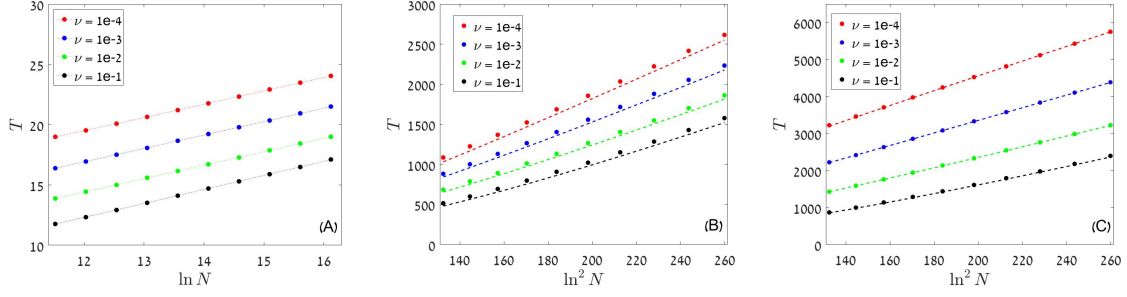


FIG. 5: The time to extinction as a function of N at the transition between the inactive (logarithmic) phase and the power-law region, $r_0 = 0$, for finite environmental stochasticity $\tilde{\sigma} = 0.21$ and $\tau = 1.25$. Different colors correspond to different ν s, see legend. Points were obtained from a numerical solution of Eqs. (5), dashed lines are analytic solutions. Panel A (left) provides the results for a single mutant ($n(t=0) = 1$). Here Eq. (40) does not give the exact numbers because of discretization effects, still the linear dependence on $\ln N$ is observed, as demonstrated by the dotted straight lines, plotted only to guide the eye. In panel B (middle), $n(t=0) = \sqrt{N}$ and the dashed lines represent the predictions of Eq. (39), the agreement is very good. In panel C (right) the results for maximal capacity $n(t=0) = N$ are compared with the predictions of Eq. (42) (dashed) and the agreement is perfect

$T(x)$ may be calculated [up to a constant, which is $T(1)$] in a different way, by integrating T'_{out} from 1 to x . With the definition $q \equiv (\nu t)/g(1-t)$ one gets, when $x \ll 1$

$$\frac{1}{g} \int_{\infty}^{(\nu x)/g(1-x)} \frac{e^q}{gq} Ei(q) dq \approx -\frac{1}{4g} (2\gamma_E^2 + \pi^2 + 4\gamma_E \ln \nu/g + 2\ln^2 \nu/g - 4[\gamma_E + \ln \nu/g] \ln x + 2\ln^2 x).$$

Subtracting this from Eq. (39) one gets the time to extinction at maximal capacity,

$$T(1) = \frac{1}{4g} (2\gamma_E + 5\pi^2/2 + 4\gamma_E \ln \nu/g + 2\ln^2 \nu/g - 2[2\gamma_E + 2\ln \nu/g - \ln G] \ln G). \quad (42)$$

See Fig. 5, panel (C).

VII. CRITICAL SYSTEM WITH PURE DEMOGRAPHIC NOISE

To provide a comprehensive outlook, we would like in this section to calculate the mean time to extinction at the transition point for a system under pure demographic noise, $r_0 = g = 0$.

Eq. (10) now takes the form,

$$\frac{1}{N} T'' - \frac{\nu x}{1-x} T' = -\frac{1}{x(1-x)}. \quad (43)$$

In the inner regime where $1-x \approx 1$ we can write,

$$\begin{aligned} T''_{in} - N\nu x T'_{in} &= -\frac{N}{x} \quad T_{in}(0) = 0 \\ \left(T'_{in} e^{-N\nu x^2/2} \right)' &= -N \frac{e^{-N\nu x^2/2}}{x} \\ T_{in} &= c_1 \int_0^x e^{N\nu t^2/2} dt + \sqrt{\frac{N}{8\nu}} \int_0^{N\nu x^2/2} \frac{e^z Ei(z)}{\sqrt{z}} dz. \end{aligned} \quad (44)$$

In the outer regime $N\nu x \gg 1$, T'' is negligible and both the remaining equation and the boundary condition at $x = 1$ are satisfied by,

$$T'_{out} = \frac{1}{\nu x^2}. \quad (45)$$

Accordingly,

$$T_{out} = c_2 - \frac{1}{\nu x}. \quad (46)$$

To match T_{in} with T_{out} c_1 has to vanish since the first integral in the last line of (44) diverges in the limit $N\nu x \rightarrow \infty$. Evaluating the large $N\nu x^2/2$ limit of the other integral one finds that

$$c_2 = \sqrt{\frac{N\pi^3}{8\nu}},$$

so the mean time to extinction, starting at $x = 1$, is

$$T_{out}(x=1) = \sqrt{\frac{N\pi^3}{8\nu}} - \frac{1}{\nu}. \quad (47)$$

This agrees with the result obtained by [24] and with the numerics (panel (E) of Fig. 6).

On the other hand, the time to extinction for a single mutant is obtained by plugging $x = 1/N$ in T_{in} ,

$$T(1/N) = 1 - \frac{\gamma_E + \ln(\nu/2) - \ln(N)}{2}. \quad (48)$$

Panel (A) of Fig. 6 demonstrated the accuracy of this approximation.

In general, when $x \sim N^{-\beta}$ where $1/2 \leq \beta \leq 1$, the time to extinction scales like

$$T \sim N^{1-\beta} [C_1 + C_2 \ln(N^{2\beta-1})], \quad (49)$$

where C_1 and C_2 are some constants. The fit of this formula to numerical results (panels B-D of Fig. 6) is very good.

VIII. FAILURE OF THE CONTINUUM APPROXIMATION AND A WKB APPROACH

The analysis so far suggests that when $r_0 > 0$ the time to extinction grows like $N^{r_0/g}$. This cannot be a general statement. In systems with pure demographic stochasticity it is already known that T grows exponentially with N when $r_0 > 0$ and N is taken to be large [1, 18, 25]. If $\sigma < r_0$ the system jumps between two states, both with positive growth rate, so even in the worst case scenario, when it is stacked for a long time in the negative σ state, the time to extinction is still exponential in N . Accordingly, the power law behavior must cross over to an exponential behavior when $r_0 \rightarrow \sigma$.

This simple argument points out to the collapse of the continuum approximation presented above. When the continuum approximation holds, the characteristics of the system depend on $g = \sigma^2\tau/2$, which is the effective diffusion constant in log-abundance space. Conversely, when the system reaches the point where $\sigma = r_0$ its qualitative behavior changes dramatically, since now the linear growth rate is always positive and extinction happens only due to demographic noise. This feature is independent of the value of τ , meaning that the diffusion approximation must break down somewhere inside the power-law region.

To analyze the system when the continuum approximation fails, we adopt a version of the WKB analysis presented and discussed in [18, 26]. We shall neglect the demographic noise and replace it (as in [1, 7]) by an absorbing boundary condition at $x = 1/N$.

We begin with our logistic equation,

$$\dot{x} = (r_0 \pm \sigma)x - (s_{eff} \pm \sigma)x^2, \quad (50)$$

and assume that the environment stays in the same state (plus or minus σ) for $\tilde{\tau}$ generations and then switches, with probability 1/2, to the other state (minus or plus σ). Note that until now the sojourn times were taken from an exponential distribution with mean τ ; below we will explain the relationships between $\tilde{\tau}$ and τ .

From Eq. (50) one finds that, if the system reaches x at certain time t , then one time increment before, i.e., at $t - \tilde{\tau}$, it was either at $\ell_+(x)$ or $\ell_-(x)$ where,

$$\begin{aligned} \ell_+ &= \frac{x_+^*}{\left(\frac{x_+^*}{x} - 1\right) e^{\tilde{\tau}(r_0+\sigma)} + 1} \\ \ell_- &= \frac{x_-^*}{\left(\frac{x_-^*}{x} - 1\right) e^{\tilde{\tau}(r_0-\sigma)} + 1}, \end{aligned} \quad (51)$$

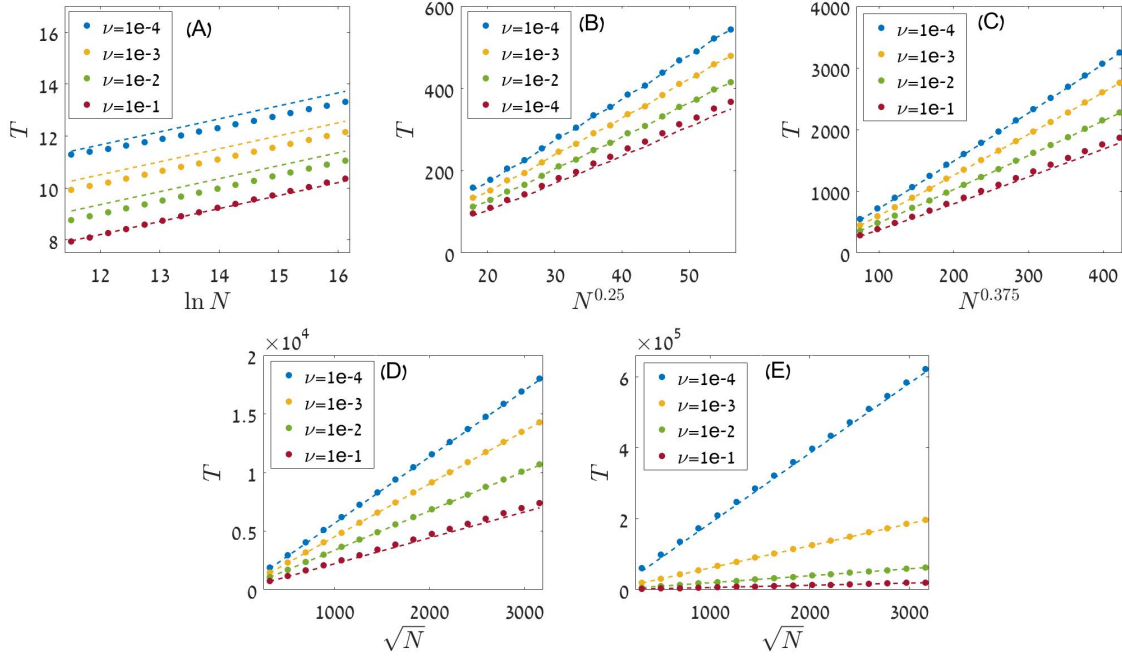


FIG. 6: Time of extinction as function of N where $r_0 = 0$ without environment stochasticity ($\tilde{\sigma} = 0$). Points were obtained from a numerical solution of Eqs. (5). Panel A provides the results for a single mutant ($n(t=0) = 1$), the dashed lines represent the corresponding predictions of Eq. (48). Panels B-D provides the results for $n(t=0) = N^{-\beta}$ where $\beta = 0.75$ (panel B), $\beta = 0.625$ (panel C) and $\beta = 0.5$ (panel D). the dashed lines represent the corresponding predictions of Eq. (49) with $C_1 = 1 - (\gamma_E + \ln \nu/2)/2$ and $C_2 = 1/2$. Panel E provides the results for maximal capacity ($n(t=0) = 1$), the dashed lines represent the corresponding predictions of Eq. (47). The constants C_1 and C_2 calculated by approximate T'_{in} (Eq. 44) for $x^2 \ll 1/N\nu$.

and the quantity

$$x_{\pm}^* = 1 - \nu/(s_{eff} \pm \sigma),$$

is the nonzero fixed points of the plus and the minus state, correspondingly. When $r_0 < \sigma$ the value of x_- is non physical, either below zero or above one, but ℓ_- is between zero and one.

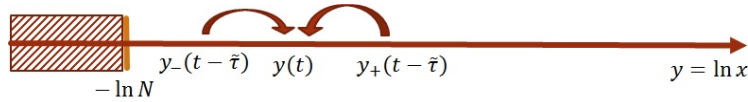


FIG. 7: An illustration of the dynamics considered using the WKB approximation. The dynamics takes place on the $y = \ln x$ axis, and the chance of the system to be at y when the time is t is completely determined by its chance to be at y_{\pm} at $t - \tau$. The values of y_{\pm} are calculated from the deterministic equation 50, without taking demographic stochasticity into account, so there are only two initial conditions that map to $y(t)$ - each correspond to one state of the environment. Without demographic noise, this dynamics yields a stable probability distribution function $P(y)$ if $r_0 > 0$. The only effect of demographic noise that we take into account is the possibility of extinction, which is proportional to the support of $P(y)$ on the extinction zone $x < 1/N$, or $y < -\ln N$.

Now let us define $y \equiv \ln x$ and $y_{\pm} \equiv \ln \ell_{\pm}$. The probability to find the system at the log-density y at time t , $P(y, t)$ satisfies the master equation,

$$\frac{dP(y, t)}{dt} = \frac{1}{2} [-2P(y) + P(y_+) + P(y_-)]. \quad (52)$$

As in [18], we assume the existence of a quasi stationary probability distribution function $P(x)$. Although the system "leaks" to extinction from the state with one individual, we consider this leak to be extremely weak, so the system equilibrates to its quasi steady state on timescales that are much shorter than the mean time to extinction

(see Figure 7). This allows one to solve Eq. (52) neglecting $dP/dt \approx 0$. The rate of extinction is then estimated from the probability to find the system with one individual, i.e., to be in the region $0 < x < 1/N$, or $-\infty < y < -\ln N$,

$$\text{Rate} \sim \int_{-\infty}^{-\ln N} P(y) dy,$$

and the mean time to extinction is the inverse of this rate. The large- N asymptotics of the extinction rate depends only on the small- x asymptotics of the quasi-stationary probability function, the behavior of $P(y)$ at larger y -s determines only the normalization factor, but this factor is independent of N .

In the extinction regime x is vanishingly small and $\ell_{\pm} \approx x e^{-\tilde{\tau}(r_0 \pm \sigma)}$. Accordingly, for $x \ll 1$ the quasi-stationary state satisfies,

$$P(y - \tilde{\tau}[r_0 + \sigma]) + P(y - \tilde{\tau}[r_0 - \sigma]) = 2P(y). \quad (53)$$

Now we implement a WKB approach. Instead of expanding $P(y_{\pm})$ to second order in Δy (this will give us the continuum Fokker-Planck equation and the power-law behavior of the continuum limit) we expand the logarithm of P in small Δy . The breakdown of the continuum approximation suggests that P_n varies significantly over the integers, so the approximation $P(x + 1/N) \approx P(x) + P'/N + P''/(2N^2)$ fails. Still, the logarithm of P may be a smooth enough function.

Accordingly, we write $P(y) = e^{S(y)}$ and implement the continuum approximation to S , replacing $S(y + \Delta y)$ by $S(x) + \Delta y S'(x)$, so $S'(x)$ is obtained as a solution of the transcendental equation

$$\exp(-\tilde{\tau} r_0 S') \cosh(\tilde{\tau} \sigma S') = 1. \quad (54)$$

This equation does not depend on y , so $S' = q$ where q is some constant. Accordingly $S \sim qy$, so $P \sim \exp(qy)$, the rate satisfies $\text{Rate} \sim N^{-q}$ and the time to extinction behaves like

$$T \sim N^q.$$

When $r_0 \ll \sigma$ one expects $q \ll 1$. When this is the case both $q\tilde{\tau}r_0$ and $q\tilde{\tau}\sigma$ are small numbers and Eq. (54) yields,

$$q = \frac{2r_0}{(\sigma^2 + r_0^2)\tilde{\tau}} \approx \frac{2r_0}{\sigma^2\tilde{\tau}}, \quad (55)$$

where the last approximation reflects a self consistency requirement for $q\tilde{\tau}r_0 \ll 1$. On the other hand if $q\tilde{\tau}\sigma$ is large,

$$q = \frac{\ln 2}{\tilde{\tau}(\sigma - r_0)}. \quad (56)$$

The case (55) corresponds to the regime where the continuum approximation holds. In that case the typical history that takes the system to extinction is a random walk in the log-abundance space (see discussion in Section X and in particular Figure 13). To translate $\tilde{\tau}$ to the parameter τ with which our model was defined in the former sections, one has to compare the variance of the sum of M steps of length $\tilde{\tau}$ and random direction, with the variance of the sum of M numbers picked independently from an exponential distribution with mean τ , half of them with plus sign and half with a minus sign. This implies that $\tilde{\tau} = \tau$ and

$$T \sim N^{r_0/g}, \quad (57)$$

as expected.

In the other extreme, Eq. (56), extinction occurs due to a (rare) long sequence of bad years, so $\tilde{\tau}$ must be compared with the tail of the corresponding exponential distribution, in which case $\tilde{\tau} = \tau \ln 2$, hence

$$T \sim N^{\frac{1}{\tau(\sigma - r_0)}}, \quad (58)$$

so the time diverges as $r_0 \rightarrow \sigma$, as suggested above.

Beside these limits, The transcendental equation (54) has to be solved numerically. In figure 8 these numerical solutions are compared with the results obtained from a numerical solution of the BKE and with the asymptotic expressions (57) and (58).

This WKB analysis covers the power-law regime where the linear growth rate may become negative and the time to extinction is related to the chance for a sequence of bad years. The procedure breaks down at $\sigma = r_0$. Above this point there are no bad years anymore and extinction happens only due to demographic stochasticity, as discussed in the next section.

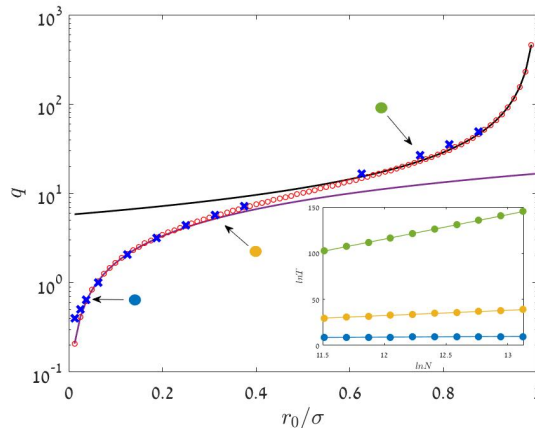


FIG. 8: In the temporal Griffiths phase $T \sim N^q$. The main panel shows q vs. r_0/σ as obtained from numerical solution of Eq. (54) (red open circles), in comparison with the asymptotic expressions for the diffusive regime [Eq. (57), purple line] and in the large r_0 regime [Eq. (58), black line]. In the inset we present results for $T(N)$ as obtained from the numerical solution of the exact backward Kolomogorov equation for $r_0 = 0.003$ (blue circles) 0.025 (yellow) and 0.06 (green). By fitting these numerical results (full lines) one obtains the actual power q , and the outcomes are represented by blue Xs in the main panel (the Xs that correspond to the three specific cases depicted in the inset are marked by arrows in the main panel). In general the predictions of the WKB fit quite nicely the numerical outcomes, and the slight deviations in the low r_0 region are due to the prefactors of the power law, and in these cases the numerical $T(N)$ graph fits perfectly the predictions of Eq. (28). All the results here were obtained for $\sigma = 0.08$, $\tau = 3/2$, $\nu = 0.04$.

IX. THE POWER-LAW-EXPONENTIAL TRANSITION AND THE EXPONENTIAL PHASE

When the linear growth rate is positive and $\sigma = 0$ (no environmental stochasticity) extinction still take place due to demographic noise, but the time to extinction grows exponentially with N . This problem has been considered recently by many authors [25, 27, 28]. Here we would like to present a brief qualitative discussion of the effect of environmental variations in this exponential phase, i.e., when $\sigma < r_0$ so the linear growth rate is always positive.

To begin, let us consider the transition points between the power-law and the exponential phase, i.e., the line $\sigma = r_0$ in Figure 1. For lower values of r_0 the linear growth rate may become negative while for higher values the linear growth rate is always positive. At the transition the system fluctuates between two states, in one of them the linear growth is positive and the time to extinction is exponential in N , while in the other state the linear growth rate is zero.

As we have shown in section VII, when the environment does not fluctuate and the linear growth rate is zero (the transition point $r_0 = 0$, $\sigma = 0$ at the origin of Fig. 1) the time to extinction, when the initial fraction of the population is $\mathcal{O}(1)$, scales like the square root of N . Accordingly, the most plausible route to extinction, for system that jumps between $r_0 + \sigma = 0$ and $r_0 + \sigma > 0$, is a sequence of $\mathcal{O}(\sqrt{N})$ marginal years, an event that occurs with probability $\exp(-\sqrt{N}/\tau)$. The rate of extinction in the positive growth state decays exponentially with N , so it is subdominant in the large N limit. Given that, at the transition point one expects a stretched exponential behavior of the time to extinction

$$T \sim e^{\sqrt{N\pi^3/8\nu}}. \quad (59)$$

As seen in Figure 9, the behavior is indeed stretched exponential $T \sim \exp(N^\gamma)$ but $\gamma \approx 0.37$. We believe that this deviation has to do with the full probability distribution function $f(T)$ in the purely demographic neutral case. Apparently this distribution admits exponential tails that lead, when convoluted with the factor $\exp(-T/\bar{\tau})$, to moving maximum in the corresponding Laplace integral that yields this value of γ .

A similar argument is relevant above the transition zone. In this case the system jumps between two states, both of them with positive growth rate. The rate of extinction in both states scales like $\exp(-\alpha N)$, but the coefficient α is larger in the plus state (linear growth rate $r_0 + \sigma$) and smaller in the minus state (linear growth rate $r_0 - \sigma$). When extinction happens due to demographic noise, the duration of the extinction event (expected duration of the final decline, [1]) scales like $\ln N/(r_0 \pm \sigma)$. Accordingly, the dominant route to extinction involves a period $\ln N/(r_0 - \sigma)$ in which the system stays in the minus state. The chance to pick such a period is $N^{-1/\tau(r_0 - \sigma)}$, so it contributes only a power-law correction to the $\exp(-\alpha N)$ factor. All in all, in the large N limit the time to extinction in fluctuating environment converges to the time to extinction of the minus state, up to power-law corrections.

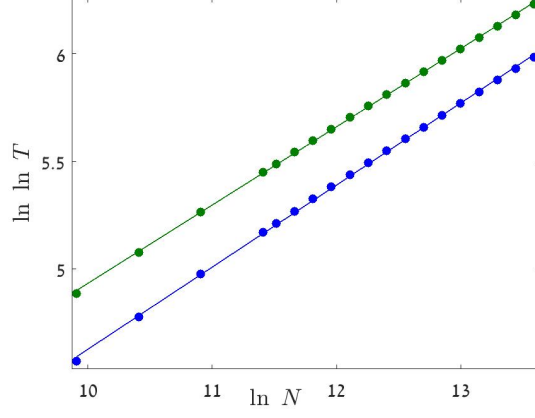


FIG. 9: Stretched exponential relationships between the mean time to extinction T and the carrying capacity N at the Griffiths-exponential transition point $r_0 = \sigma$. $\ln \ln T$, as obtained from numerical solutions of the BKE (filled circles), is plotted against $\ln N$ and the linear fits (straight lines) suggest slopes around $\gamma \approx 0.37$. Parameters are $\tau = 1$, $\bar{\sigma} = 0.4$ and $\nu = 0.2$ (green), 0.1 (blue).

X. PROBABILITY DISTRIBUTION FUNCTION FOR THE TIME TO EXTINCTION

Until now we have calculated the mean time to extinction, T , in the various phases of the logistic system. Here we would like present a few considerations regarding the full probability distribution function for extinction at t , $f(t)dt$, or the survival probability $Q(t)dt$. Of course

$$f(t) = -dQ(t)/dt.$$

The state of our system is fully characterized by $P_{e,n}(t)$, the chance that the system admits n A particles at t , when the environmental state is e (for dichotomous noise e takes two values that correspond to $\pm\sigma$). After a single birth-death event (time incremented from t to $t + 1/N$), the new state is given by

$$P_{e,n}^{t+1/N} = \mathcal{M} P_{e',m}^t, \quad (60)$$

where \mathcal{M} is the corresponding Markov matrix. Its matrix elements $\mathcal{M}_{e,n;e',m}$ are the chance to jump from m particles in environment e' to n particles in environment e . These elements were given in Eqs. (4) above.

The highest eigenvalue of the Markov matrix, $\Gamma_0 = 1$, corresponds to the extinction state, i.e, to the right eigenvector $P_{e,n} = \delta_{n,0}$ (at extinction the state of the environment is not significant) or the left eigenvector $(1, 1, 1, \dots)$. Using a complete set of left and right eigenvectors of this kind one may write $P_{e,n}(t)$ as,

$$P_{e,n}(t) = \sum_k a_k v_k (\Gamma_k)^{Nt}. \quad (61)$$

Here the index k runs over all eigenstates of the Markov matrix, v_k is the k -s right eigenvector, a_k is the projection of $P_{e,n}(t=0)$ on the k -s left eigenvector and Nt is the number of elementary birth-death events at time t (for $t = 1$, i.e., a generation, $Nt = N$).

Writing $\Gamma_k = |\Gamma_k| \exp(i\phi_k)$, one realizes that each k mode decays like $\exp(-Nt\epsilon_k)$, when $\epsilon_k \equiv -\ln|\Gamma_k|$. Since the Markov matrix is real, eigenvalues are coming in complex conjugate pairs so P_n is kept real and non negative at any time. For the extinction mode $\epsilon_0 = 0$, all other modes have $\epsilon_k > 0$

Clearly, for any finite system the subdominant mode ϵ_1 determines the maximal persistence time of the system, so at timescales above $t = 1/N\epsilon_1$ the chance of the system to survive, $Q(t)$, decays exponentially with t .

Now one would like to make a distinction between two different situations. In the first, there is a *gap* between ϵ_1 and ϵ_2 , so when $N \rightarrow \infty$ $\epsilon_1 \ll \epsilon_2$. This behavior is demonstrated in the right panels of Figures 10 and 11 and in Figure 12. In such a case the large t behavior of the system is simply

$$Q(t)dt = \exp(-t/t_0), \quad (62)$$

where

$$t_0 \equiv 1/N\epsilon_1. \quad (63)$$

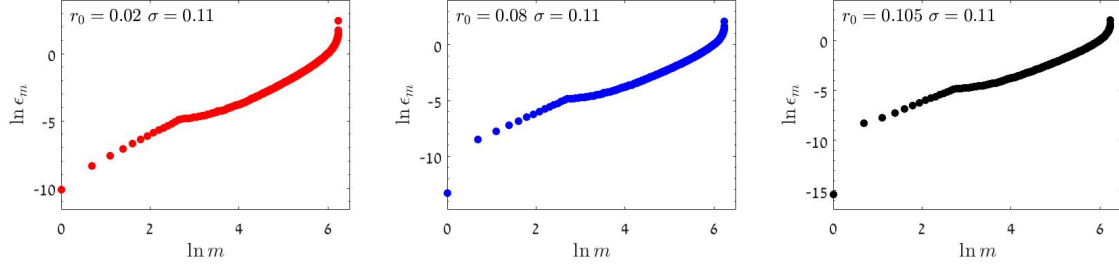


FIG. 10: The logarithm of the absolute value of the eigenvalues of the Markov matrix, ϵ_m , is plotted against $\ln m$ for small r_0 (left panel), intermediate r_0 (middle panel) and large r_0 (right panel). The state with $m = 1$ ($\ln m = 0$) is the most persistent non-extinction state. Clearly, as r_0 increases, a gap is opened between ϵ_1 and ϵ_2 (see figure 9). For $m > 1$, the low-lying states satisfy $\epsilon_m \sim m^\rho$, where $\rho \approx 1.7$. Parameters are $\tau = 1$, $\nu = 0.1$ and $N = 2^8$.

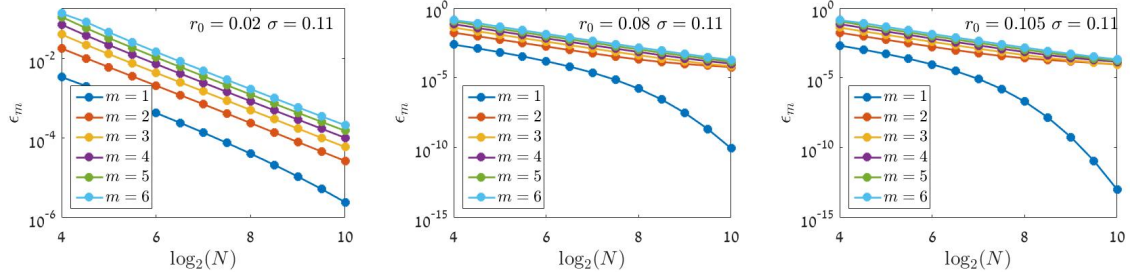


FIG. 11: ϵ_m (from $m = 1$ to $m = 6$, see legends) is plotted against $\log_2 N$ for different values of r_0 . Parameters are $\tau = 1$ and $\nu = 0.1$.

Accordingly, $f(t) = -\dot{Q} = \exp(-t/t_0)/t_0$ and the mean time to extinction $T = t_0 = 1/N\epsilon_1$.

In the exponential phase the situation corresponds to this gap scenario, as discussed in [18]. The purely exponential distribution (62) reflects an absence of memory: the system sticks for long times to its quasi stationary state v_1 , and decay to zero on much shorter timescale due to rare events. The decline to extinction may be a result of a rare demographic event, like an improbable series of individual death, or the result of an environmental rare event - an improbable series of bad years. In both cases, the *decline time* (as defined in [1]) is short (logarithmic in N), so the exponential distribution reflects the accumulated chance of rare, short, and independent catastrophes. This *sharp decline* behavior is demonstrated in the right panel of Fig. 13.

The second scenario (demonstrated in the left panel of Figs 10 and 11 and in the blue line of Fig 9) correspond to a *gapless* system. Here the eigenvalues of \mathcal{M} satisfy $\epsilon_m \sim \epsilon_1 + c_1(m-1)^\rho$, where c_1 is some tiny constant. In such a case the $\exp(-tN\epsilon_1)$ factors out of the sum (61), and the rest of the sum may be approximated by $\int \exp(-c_1 t N m^\rho) dm$, yielding a power-law decay so,

$$Q(t)dt \sim \frac{e^{-t/t_0}}{(Nt)^{1/\rho}} dt. \quad (64)$$

In that case the mean time to extinction is not exactly t_0 but the difference is only a numerical factor. If $\rho > 1$ then,

$$T = t_0(1 - 1/\rho), \quad (65)$$

while if $\rho < 1$ the ratio between T and t_0 depends on the short time cutoff that must be imposed on the distribution (X) to avoid divergence at zero.

This *soft decline* is not purely exponential, since the system has long-term memory. Rare catastrophic events put an upper bound on the lifetime of the population, but extinction may occur, with relatively high probability, due to the random walk of the population size along the log-abundance axis.

In Figure 13 we show a typical trajectory in each regime, together with a sketch of the right eigenvector (that corresponds to ϵ_1) for the given r_0 values. In the gap regime the overlap of the quasi-stationary state with the extinction point is small and a typical trajectory fluctuates around x^* (the point where the mean of \dot{x} vanishes, where the average is taken over the two signs of σ), where the amplitude of fluctuations is much smaller than x^* . Accordingly, the decline time is relatively short. On the other hand in the gapless case the fluctuation amplitude is larger than x^* and the decline time is comparable with the lifetime.

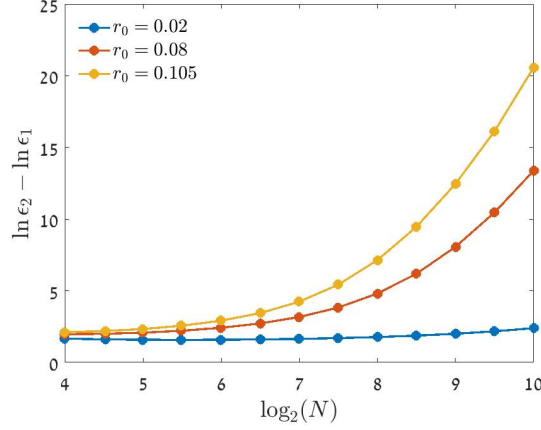


FIG. 12: The gap, $\ln \epsilon_1 - \ln \epsilon_2$, as a function of $\log_2 N$. As N increases the gap grows when r_0 is large or intermediate but remains more or less fixed when r_0 is small. Parameters are $\tau = 1$ and $\nu = 0.1$.

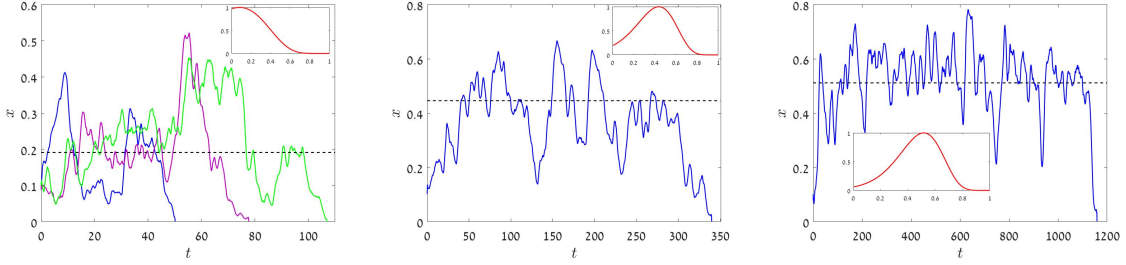


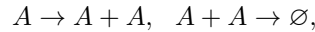
FIG. 13: In the main panels, typical trajectories are shown for a system with $\tau = 1$, $\sigma = 0.11$ and $\nu = 0.1$, for $r = 0.02$ (left), 0.08 (middle) and 0.105 (right). The dashed line corresponds to x^* , the point where the mean (over environmental conditions) growth rate is zero. In the insets the most stable right eigenstate is plotted for each case. For large r_0 the quasistationary state is peaked far from the extinction point, so the trajectory fluctuates in a relatively narrow band around x^* . The final decline is sharp: extinction happens due to the accumulation of rare sequences of bad years, and the timescale associated with the decline time is microscopic (in fact, this timescale is logarithmic in N while the lifetime grows like a power law in N). As r_0 becomes smaller (the gapless scenario) the fluctuations are comparable with x^* , hence the decline time becomes a finite fraction of the lifetime (soft decline).

XI. UNIVESALITY

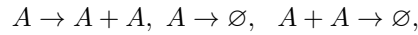
Through this article we considered one specific microscopic model, namely two species competition with one sided mutation, a classical population-genetics problem taken from [23]. Beside its concrete importance, this system is technically more tractable since it corresponds to a zero sum game so the total community size N is strictly fixed and still the system shows negative density dependence.

What about other microscopic processes that yield, in their deterministic limit, a transcritical bifurcation? It is widely believed that, although some details may depend on the microscopcy of the process, the main characteristics of the behavior: the different phases, the functional N dependence in each phase, and the behavior at the transition points - are *universal*, i.e., are independent of the microscopcy.

For example, in [18] the mean time to extinction of the two processes



and



was calculated. Both these processes are logistic, and under pure demographic stochasticity T grows like $\exp(\alpha n^*)$, where n^* is the number of individuals in the quasi-stationary state. The value of α does depend on the microscopcy and the two different models yield different α -s, but the exponential growth of T with n^* is a universal feature.

Accordingly, in our case one may expect, for different microscopic models, the same phase diagram with exponential, power-law and logarithmic regimes, but the prefactors and the constants may differ.

In the literature one may find other models that belong to the equivalence class of the logistic growth with environmental stochasticity. These include a model with ceiling (i.e., for which the growth rate is density-independent until it reaches a prescribed value n^* , where reflecting boundary conditions are imposed [1, 29] or simple logistic equation [19, 22]. Indeed for these models the authors obtained the same N dependence that we obtained here when the diffusion approximation holds (to the left of the dashed line in Fig. 1).

Moreover, the WKB analysis presented in Section VIII allows us to suggest a much stronger statement.

As explained, the chance of extinction, and the associated timescale, are given by the behavior of $P(x)$ at $x < 1/N \ll 1$ (Rate $\sim \int_0^{1/N} P(x) dx$). This behavior is determined, in turn, by the small x dependency of ℓ_+ and ℓ_- . To satisfy Eq. (54) above, r_0 must be positive, and this implies that $|\ell_+ - x| > |\ell_- - x|$, i.e., that the mean growth rate of the species, when rare, is positive. This is a sufficient condition for the validity of the WKB analysis presented above, independent of the details of the model at larger x -s.

Accordingly, our WKB analysis shows that for *any* biological species, the time to extinction is a power-law in N when the following conditions are met:

- The probability distribution function $P(x)$ is normalizable (this condition excludes the logarithmic phase, and ensures that the N -dependency comes only from the behavior of $P(x \ll 1)$).
- The dynamics allows for periods of growth and periods of decline (this condition excludes the exponential phase).
- When the focal species is rare ($x \ll 1$), its time-averaged growth rate is positive ($|\ell_+ - x| > |\ell_- - x|$).
- When the focal species is rare it grows exponentially during periods of positive growth rate.

XII. PRACTICAL IMPLICATIONS

The dynamics of a single population is the basic building block of many theories in population genetics, ecology and evolution. As in almost any realistic situation environmental fluctuations plays a major role in system's dynamics, one expects that the phase diagram presented here may shed a new light on the analysis of empirical data in these fields. In this section we would like to sketch of a few emerging insights.

A. Population viability analysis

Population viability analysis [1, 29–31] is a method of risk assessment frequently used in conservation biology. Its main aim is to determine the probability that a population will go extinct within a given number of years. In the typical case the empirical data is abundance timeseries (the number of birds or nests observed at a certain place, the number or the biomass of conspecific trees or shrubs in a region). In some cases these timeseries are collected over a few decade (for example, the North American Breeding Birds survey (NABBS) has now almost 50 years of large scale censuses).

To extract information, and to suggest predictions based on these timeseries, one would like to analyze them using a decent model. In general a given timeseries is used to infer model parameters and to estimate the strength of stochasticity, then one uses the calibrated model to predict long-term dynamics.

The models used for PVA are almost always logistic or logistic like, so the maximum abundance of a viable population is limited by a certain density-dependent mechanism. The general form of these models is $\dot{x} = R(x)x$, where $R(x)$, the per-capita growth rate, is a monotonously decreasing function of x that reaches zero at x^* , the stable fixed point. In the logistic model $R(x)$ decays linearly with the population size, in a ceiling model the growth rate is fixed until the population hits the carrying capacity ($R(x) = r_0$ for $x < x^*$ with reflecting boundary conditions at x^*), and in Ricker model the birth rate decays exponentially with the population size until it becomes equal to the death rate. The models may differ in some details and may admit discrete time maps ($x_{t+1} = R(x_t)x_t$) but they all belong to the transcritical bifurcation class. Table 1 of [31], for example, provides references to 27 works in which these models have been used.

However, the predictions of population viability analysis of this kind may be problematic. It is very difficult to estimate the model parameters from empirical timeseries, and on the other hand the results are in many cases very sensitive to these parameters [32]. The analysis suggested here emphasizes *universal*, model independent aspects of the dynamics and we would like to suggest our phase diagram as an alternative classification scheme for viability analysis. Instead of trying to predict the chance of extinction, one would like to adopt a more qualitative approach and to

classify populations by their stability properties (the three regimes in Fig. 1) and their decline modes (left/right to the dotted-dashed transition line).

As an example, let us consider the analyses of [33, 34]. In Figure 14 we reproduce the relevant datasets from these two papers. In both datasets the chance of survival Q , or the chance of extinction $1 - Q$, after a fixed time interval (10 or 80 years) are plotted against the initial population size.

As one can see, both datasets (which are, of course, quite noisy because of the small number of samples in each bin, especially for the high abundance bins) allow for reasonable fits if the chance of survival, $Q(t)$, satisfies

$$Q(t) = \exp(-t/\tilde{\tau}N^q), \quad (66)$$

which is the expression one expects if the system is in the temporal Griffith phase. Note that the distinction between soft and sharp decline is irrelevant here, since the time window is fixed and we are interested only in the N dependence.

When we tried to fit the data with $Q = \exp(t/\tilde{\tau} \exp(\alpha N))$, as expected in the exponential phase, we ran into difficulties. In such a case one expects a much steeper dependence of Q on N : if $T \sim \exp(\alpha N)$ than when N varies from $0.1/\alpha$ to $10/\alpha$, say, Q varies from vanishing values to one, so the survival probability is a sharp sigmoid unless α takes very small values. As a result, we have failed to fit the datasets with exponential dependency unless α was taken to be extremely small ($\alpha \sim 0.01$).

Moreover, both studies did not report a significant abundance decline in the surviving populations - in most of them abundance either grew up or kept fixed, see Figure 4 of [34] and Figure 4 of [33]. This implies that both systems are not in the logarithmic phase, where one should expect a general decrease in abundance for all populations.

Accordingly, it seems that a consistent interpretation of the observed data suggests that the surveyed bird and plant populations are in the temporal Griffith phase, where the lifetime of a population scales N^q , with q values between 0.3 and 0.5.

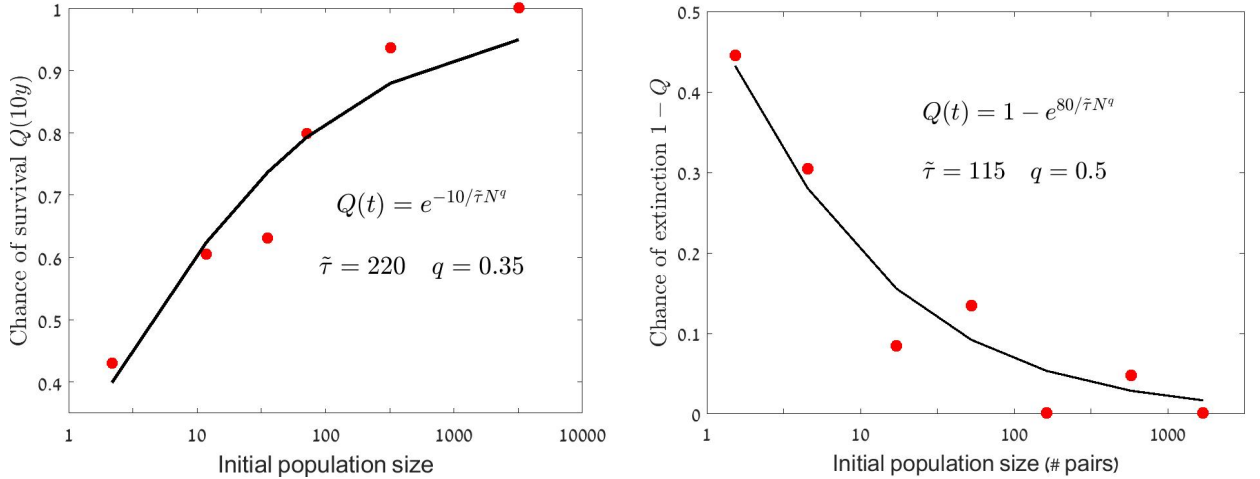


FIG. 14: The left panel (Figure 1 of [33]) shows the relationships between the size of plant populations in 1986 and their chance to survive 10 years later (red circles). The black line is the best fit to $Q(t)$, assuming that the mean time to extinction T growth like N^q . In the right panel we retrieved Figure 5 of [34], and the red circles correspond to the chance of extinction of birds populations vs. the initial number of pairs (the last point in the original figure, that was too close to zero to be digitised, was omitted). The black line is the best fit to $1 - Q(t)$, assuming that the mean time to extinction T growth like N^q .

Similar conclusions are suggested by the work of Ferraz et al [35], who measured the rate of bird species loss in amazonian forest fragments as a function of fragment area. If we assume that the initial population size is proportional to the area of the fragment, and that within each fragment the population is more or less well mixed (perhaps a reasonable assumption for birds), the scaling of extinction times with fragment area is the same as the scaling of extinction time with population size. The authors of [35] reported that “A 10-fold decrease in the rate of species loss requires a 1,000-fold increase in area”, suggesting $q \approx 1/3$. However, large fragments may contain more low-density species to begin with, so the actual value of q is perhaps higher than $1/3$.

B. Conservation, management, and decline modes

The main purpose of conservation efforts is to avoid extinction of local populations. To that aim, we suggest that the distinction between soft decline and sharp decline (the two sides of the dotted-dashed line in Fig. 1) is very important.

In the soft-decline regime (including the logarithmic phase) the system faces a severe risk of extinction *and* its dynamics is strongly related to the factors that actually lead to extinction, like grazing or fishing or climate change and so on. In this regime one would like to identify these factors and, if possible, to avoid them.

The situation is completely different in the sharp decline regime, where the system fluctuates for a long time around an equilibrium value and extinction is caused by rare events (a long series of bad years, for example). Predicting rare events from a given, relatively short, timeseries is usually a lost cause, so one would like to direct conservation efforts in other directions.

Decline modes may be inferred from the statistics of extinction events in timeseries, provided that false extinction events (due to sampling errors) are filtered out somehow. Large scale empirical studies of $Q(t)$ (like those presented in [36, 37], based on the NABBS data) suggest an exponentially truncated power law. If one likes to interpret these results as reflecting purely local logistic-like dynamics under environmental stochasticity (this was not the interpretation given in [37] - they considered a neutral model with immigration), it implies that the decline mode in these systems is indeed soft.

C. Spatial effects

One of the main obstacles to the understanding of ecological dynamics is the need to bridge over length and time scales. Understanding of stability developed at small scales can not be easily extended to larger scales, since the type and effect of ecological processes vary with scale. For example, the work of [35] suggests, as mentioned above, that a ten fold decrease in $t_{1/2}$ (time to lose 50% of the species) requires a 1000 fold increase in fragment size, and that $t_{1/2}$ for a fragment of 100 km² is 100 years. This observation is based on a study of fragments between 0.01 and 100 km². Extrapolating this scaling law to the whole tropical south America subregion ($1.4 \cdot 10^7$ km²) yields a mean lifetime of about 10,000 years for a tropical bird species, much shorter than the standard estimates from fossil data (about a million years per species).

Our discussion so far points towards the importance of the correlation length, ξ_E associated with environmental fluctuations. When the linear size of a system is much larger than this correlation length local extinctions are uncorrelated and may be compensated by recolonization of empty patches by neighboring populations (a metapopulation dynamics [38]). In that case the extinction-recolonization dynamics is some version of the contact process, and the extinction transition belongs to the directed percolation equivalence class [39]. Technically speaking, for the directed percolation transition spatio-temporal noise is an irrelevant operator that does not affect the transition exponents.

On the other hand, when ξ_E much larger than the linear size of the system temporal stochasticity is a relevant operator and the transition belongs to a different equivalence class [40]. In that case a series of bad years may kill the whole system and the chance of recolonization is small since the state of all neighboring sites is correlated. Accordingly, one expects that an increase in ξ_E makes the system less stable [41]. Upscaling of local observation is perhaps limited to length scales below ξ_E .

D. Existence and coexistence

The modern coexistence theory (MCT) have gained a lot of attention in recent years [42, 43]. The aim of this theory is to understand the conditions for coexistence of many species. Here we considered a system with only two species (and effectively one, since the game is zero-sum), still our results are relevant to one aspect (out of many) of the coexistence theory.

In MCT one analyzes the dynamics of a single species in an “effective field” that reflects both the environment and the interaction with all other species [44]. Demographic noise is not taken into account and the “existence” of a single species is related to the chance of its abundance to visit the extinction zone, which is the region between $x = 0$ and $x = \delta$. Clearly a reasonable value for δ is $1/N$ (as in Section VIII above), but the theory has no demographic stochasticity in it so δ is left arbitrary. A species coexists if, for every $\epsilon > 0$ there exists a δ such that the system spends less than ϵ of its lifetime in the extinction zone [44].

Our work shows that this is a very weak statement. For our system, the MCT persistence criteria is translated to $r_0 > 0$ (alternatively, to the divergence of T when $N \rightarrow \infty$), but in this regime the time to extinction scales like

$N^{r_0/g}$ and the exponent may take arbitrary small values ($N^{0.01}$, say), so in any realistic system the focal species will go extinct in a very short time. We believe that the distinction between sublinear and superlinear dependencies of T on N , or the decline mode, are much more important than the condition for “coexistence”.

XIII. DISCUSSION

Through this paper we considered mainly the large- N asymptotics, under the assumption that all other parameters are kept fixed and N is taken to infinity. In that case, the system allows for an exponential phase only when the noise is *bounded*. If the noise is unbounded (e.g., Gaussian noise) there is always a finite chance to pick a long series of bad years (a long period of time in which the linear growth rate is negative). This chance may be extremely tiny, but it is N -independent. As a result, it dominates the large N limit so in that limit one finds only two phases, the logarithmic phase and the temporal Griffiths phase.

Practically, the distinction between a power-law phase with diverging q and an exponential phase is, in almost any imaginable case, unimportant. We believe that in most cases the transitions, or crossovers, associated with the dotted-dashed line of Fig. 1 are much more relevant to the analysis of empirical dynamics.

Three transitions/crossovers may be identified within the temporal Griffith phase. The first has to do with the value of r_0/g . When this value is smaller than one the time to extinction is sublinear in N while above this point it is superlinear [20]. The corresponding $P(x)$ (that may be obtained from $P(y)$ that was calculated in section VIII using the appropriate Jacobian $1/x$), behaves, close to zero, like $P(x \ll 1) \sim x^{-1+r_0/g}$, so $P(x)$ changes its shape from convex to concave.

The second transition is the breakdown of the diffusion (continuum) approximation. This has to do with the dependency of P_n on n in the discrete master equation (5). When this dependency is too steep, such that gradients decay only slowly with N , the continuum approximation fails and one has to implement WKB.

A third phenomenon, discussed in Section X, is the opening of a gap in the spectrum of the Markov operator as r_0 increases. As we have seen, in a system with a gap the decline is sharp and the dynamics has no memory: during every short period of time (of order $\ln N$) the process either dies or stay alive, and persistence times have an exponential distribution. When the gap closes down the probability distribution function follows a truncated power law and extinction occurs because of the random motion along the abundance axis (soft decline).

One may wonder about the relationships between these three transitions. When $P(x)$ changes its shape from convex to concave, the fraction of time that a typical trajectory spends in the extinction zone shrinks more rapidly with N , so extinction becomes more and more associated with rare events, and this suggests that the spectrum admits a gap. Similarly, when extinction happens due to rare fluctuations associated with directed flow towards zero, it is quite plausible that the diffusion approximation breaks down, since the convergence of a binomial distribution to a Gaussian is known to fail at the far tails of the distribution. Our analysis so far do not allow us to declare that these three phenomena are all manifestations of the same transition, more work is still needed.

We acknowledge many helpful discussions with David Kessler and Matthieu Barbier. This research was supported by the ISF-NRF Singapore joint research program (grant number 2669/17).

Appendix A: Numerical methods

Through this work we compare results, obtained from numerical solutions of the backward Kolomogorov equations (BKE), to the our analytic approximations.

1. Numerical solution of the backward Kolomogorov equation

The discrete BKEs considered through this paper, (Eq. 5) is second order, linear, inhomogeneous difference equations that have the general form,

$$\begin{bmatrix} T_1^+ \\ \vdots \\ T_{N-1}^+ \\ T_1^- \\ \vdots \\ T_{N-1}^- \end{bmatrix} = \begin{bmatrix} W_{1 \rightarrow 1}^{++} & W_{1 \rightarrow 2}^{++} & \cdots & W_{1 \rightarrow 1}^{+-} & W_{1 \rightarrow 2}^{+-} & \cdots \\ \vdots & & \ddots & & \vdots & \\ \vdots & & & \ddots & & \\ W_{1 \rightarrow 1}^{-+} & W_{1 \rightarrow 2}^{-+} & \cdots & W_{1 \rightarrow 1}^{--} & W_{1 \rightarrow 2}^{--} & \cdots \\ \vdots & & \ddots & & \vdots & \\ \vdots & & & \ddots & & \end{bmatrix} \times \begin{bmatrix} T_1^+ \\ \vdots \\ T_{N-1}^+ \\ T_1^- \\ \vdots \\ T_{N-1}^- \end{bmatrix} + \frac{1}{N} \begin{bmatrix} 1 \\ \vdots \\ \vdots \\ \vdots \\ \vdots \\ 1 \end{bmatrix}, \quad (\text{A1})$$

with the W -s that were defined in Eq. (5) above. Accordingly, the values of T_n^\pm [and consequently the values of T_n and Δ_n] may be determined by inverting this $(2N-2) \times (2N-2)$ matrix and multiplying the outcome by the constant vector $-1/N$.

However, in the deep Griffith phase and in the exponential phase this procedure suffers from numerical errors, as one can see in Fig. (3). To test our WKB analysis we had to overcome this difficulty and to increase the machine precision. Wolfram's *Mathematica* provides a tempting opportunity, as it allows one to work with infinite precision variables, but is limited by its ability to invert large matrices efficiently.

To solve this problem we have implemented our numerics in *Mathematica* using a transfer matrix approach. Eq. (5) may be written as

$$\begin{bmatrix} T_n^- \\ T_n^+ \\ T_{n+1}^- \\ T_{n+1}^+ \\ 1/N \end{bmatrix} = M_n \times \begin{bmatrix} T_{n-1}^- \\ T_{n-1}^+ \\ T_n^- \\ T_n^+ \\ 1/N \end{bmatrix}, \quad (\text{A2})$$

where M_n is the transfer matrix,

$$M_n \equiv \begin{bmatrix} 0 & 0 & 1 & 0 & 0 \\ 0 & 0 & 0 & 1 & 0 \\ -\frac{W_{n \rightarrow n-1}^{--}}{W_{n \rightarrow n+1}^{--}} & 0 & 1 + \frac{W_{n \rightarrow n-1}^{--} + (\tau N - 1)/(\tau N(\tau N - 2))}{W_{n \rightarrow n+1}^{--}} & \frac{1 - \tau N}{\tau N(\tau N - 2)W_{n \rightarrow n+1}^{--}} & \frac{1 - \tau N}{\tau N W_{n \rightarrow n+1}^{--}} \\ 0 & -\frac{W_{n \rightarrow n-1}^{++}}{W_{n \rightarrow n+1}^{++}} & \frac{1 - \tau N}{\tau N(\tau N - 2)W_{n \rightarrow n+1}^{++}} & 1 + \frac{W_{n \rightarrow n-1}^{++} + (\tau N - 1)/(\tau N(\tau N - 2))}{W_{n \rightarrow n+1}^{++}} & \frac{1 - \tau N}{\tau N W_{n \rightarrow n+1}^{++}} \\ 0 & 0 & 0 & 0 & 1 \end{bmatrix}. \quad (\text{A3})$$

T may be incremented by $n+1$ abundance steps by multiplication of such matrices,

$$\begin{bmatrix} T_n^- \\ T_n^+ \\ T_{n+1}^- \\ T_{n+1}^+ \\ 1/N \end{bmatrix} = M_{n,m} \times \begin{bmatrix} T_{m-1}^- \\ T_{m-1}^+ \\ T_m^- \\ T_m^+ \\ 1/N \end{bmatrix}. \quad (\text{A4})$$

where $M_{n,m} \equiv M_n \times M_{n-1} \times \cdots \times M_{m+1} \times M_m$ (assuming $n > m$).

The transfer matrix $M_{N-1,1}$ may be used to find T_N^\pm, T_{N-1}^\pm as function of T_1^+, T_1^- , starting from the column vector $[0, 0, T_1^-, T_1^+, 1/N]$. The boundary condition equation at N (12) provide us with another pair of equations,

$$\begin{aligned} \frac{T_N^+ - T_{N-1}^+}{2} + \frac{T_N^- - T_{N-1}^-}{2} &= \frac{1}{\nu} \\ \frac{T_N^+ - T_N^-}{T_{N-1}^+ - T_{N-1}^-} &= \frac{\nu}{\nu + 2/(\tau - 2)}, \end{aligned} \quad (\text{A5})$$

which allows one to solve for T_1^+, T_1^- and to find T_n^\pm for any n by multiplying the column vector $[0, 0, T_1^-, T_1^+, 1/N]$ by $M_{n-1,1}$.

This way of using transfer matrix allows one to find T for big systems in high accuracy where only the values of the 5 transfer matrix are kept in the memory of the system.

However, because *Mathematica* adapts to the number of digits in the relevant calculation, one would like to avoid the multiplication of matrices one by one, since the number of digits in each element of the matrix increases and this consumes a lot of computer time. To allow for faster calculations, we have generated first all the transfer matrices $M_1, M_2, \cdots M_{N-2}, M_{N-1}$, then multiply all pairs of adjacent matrices and repeat the process $\mathcal{O}(\ln N)$ times to obtain $M_{n-1,1}$.

Appendix B: Dichotomous (telegraphic) and other types of noise

In this article we consider a special type of environmental stochasticity, in which the system flips between two states (good and bad years, say). Both white Gaussian noise and white Poisson noise can be recovered from this dichotomous (telegraphic) noise by taking suitable limits [45], so the results obtained here are quite generic.

As an example, if the environmental conditions are picked from a Gaussian distribution of a certain width with correlation time τ_1 , one may easily imitate these features by taking a dichotomous noise that flips between two values, $\pm\sigma$, with much shorter correlation time τ . With the appropriate choice of τ and σ , the binomial distribution of σ_{eff} , the average fitness between $0 < t < \tau_1$,

$$\sigma_{eff} = \frac{\tau_1}{\tau} \sum_i^{\tau_1/\tau} \sigma_i, \quad (\text{B1})$$

will correspond to the bulk properties of any required Gaussian noise, since the Gaussian distribution is the limit of a binomial distribution.

However, while the Gaussian distribution is unbounded, the distribution of σ_{eff} is clearly bounded; the convergence to a Gaussian takes place in the bulk but the tails are truncated.

To demonstrate the ability of a dichotomous noise to emulate the effect of other types of noise, we present in Figure 15 the outcomes of a few numerical experiments. The figures show the mean time to extinction vs. N for our two-species competition model with one sided mutation, as described in the main text [Eq. (2)]. Three types of noise are compared.

1. $s(t)$ is either σ or $-\sigma$ (dichotomous noise).
2. $s(t)$ is picked from a uniform distribution between $(-\sigma\sqrt{12})$ and $(+\sigma\sqrt{12})$.
3. $s(t)$ is picked from a beta distribution, $\text{Beta}(2, 2)\sigma/\sqrt{0.05}$.

All three distribution have a compact support, zero mean and variance σ^2 .

-
- [1] R. Lande, S. Engen, and B.-E. Saether, *Stochastic population dynamics in ecology and conservation* (Oxford University Press, 2003).
- [2] E. G. Leigh, *Journal of Evolutionary Biology* **20**, 2075 (2007).
- [3] M. Kalyuzhny, E. Seri, R. Chocron, C. H. Flather, R. Kadmon, and N. M. Shnerb, *The American Naturalist* **184**, 439 (2014).

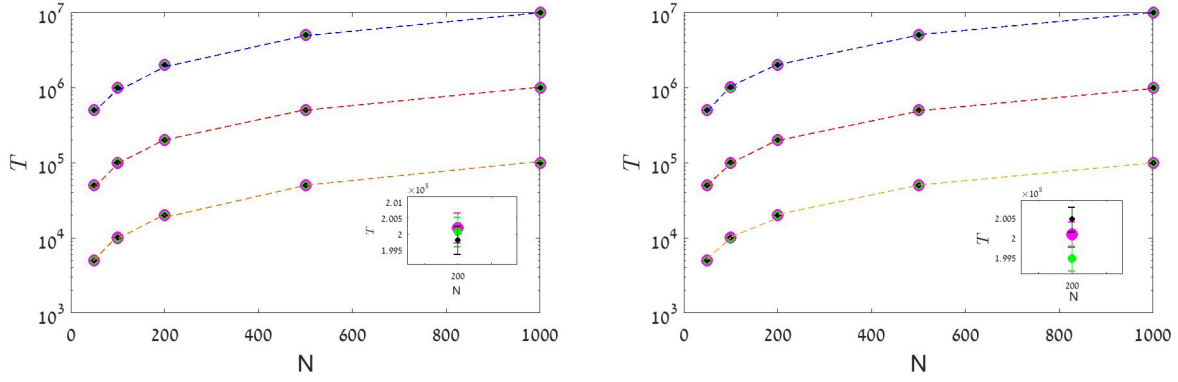


FIG. 15: Time to extinction T (log scale) vs. N for three different noise distributions. The mean (over 1000-2000 runs) time to extinction was measured as a function of $N = 50, 100, 200, 500, 1000$, for $n_0 = N$. The left panel present results for $\tau = \sigma = 0.1$ while in the right panel $\tau = \sigma = 0.3$. For each N and ν the value of T is given for dichotomous noise (green circles), uniform distribution (magenta) and Beta distribution (black). Markers were chosen with different size to improve the visibility of the results. Dashed line were added manually to guide the eye and they connect results with $\nu = 0.01$ (yellow) $\nu = 0.001$ (red) and $\nu = 0.0001$ (blue). In the insets the three points at $N = 200$, $\nu = 0.001$, with one standard deviation error bars, were magnified. These error bars are too small and cannot be seen in the main panels.

- [4] M. Kalyuzhny, Y. Schreiber, R. Chocron, C. H. Flather, R. Kadmon, D. A. Kessler, and N. M. Shnerb, *Ecology* **95**, 1701 (2014).
- [5] R. A. Chisholm, R. Condit, K. A. Rahman, P. J. Baker, S. Bunyavechewin, Y.-Y. Chen, G. Chuyong, H. Dattaraja, S. Davies, C. E. Ewango, et al., *Ecology letters* **17**, 855 (2014).
- [6] D. A. Kessler and N. M. Shnerb, *Journal of Theoretical Biology* **345**, 1 (2014).
- [7] J. Hidalgo, S. Suweis, and A. Maritan, *Journal of theoretical biology* **413**, 1 (2017).
- [8] M. Danino, N. M. Shnerb, S. Azaele, W. E. Kunin, and D. A. Kessler, *Journal of theoretical biology* **409**, 155 (2016).
- [9] M. Danino and N. M. Shnerb, *Physical Review E* **97**, 042406 (2018).
- [10] D. Kessler, S. Suweis, M. Formentin, and N. M. Shnerb, *Physical Review E* **92**, 022722 (2015).
- [11] B.-E. Sæther and S. Engen, *Trends in ecology & evolution* **30**, 273 (2015).
- [12] I. Cvijović, B. H. Good, E. R. Jerison, and M. M. Desai, *Proceedings of the National Academy of Sciences* **112**, E5021 (2015).
- [13] M. Kalyuzhny, R. Kadmon, and N. M. Shnerb, *Ecology letters* **18**, 572 (2015).
- [14] M. Danino, D. A. Kessler, and N. M. Shnerb, *Theoretical Population Biology* **119**, 57 (2018).
- [15] T. Fung, J. P. O'Dwyer, K. A. Rahman, C. D. Fletcher, and R. A. Chisholm, *Ecology* **97**, 1207 (2016).
- [16] K. Wienand, E. Frey, and M. Mobilia, *Physical review letters* **119**, 158301 (2017).
- [17] Y. Yahalom and N. M. Shnerb, *arXiv preprint arXiv:1810.03317* (2018).
- [18] D. A. Kessler and N. M. Shnerb, *Journal of Statistical Physics* **127**, 861 (2007).
- [19] A. Kamenev, B. Meerson, and B. Shklovskii, *Physical review letters* **101**, 268103 (2008).
- [20] T. Spanio, J. Hidalgo, and M. A. Muñoz, *Physical Review E* **96**, 042301 (2017).
- [21] A. H. Wada, M. Small, and T. Vojta, *arXiv preprint arXiv:1805.02583* (2018).
- [22] F. Vazquez, J. A. Bonachela, C. López, and M. A. Munoz, *Physical review letters* **106**, 235702 (2011).
- [23] S. Karlin and H. E. Taylor, *A second course in stochastic processes* (Elsevier, 1981).
- [24] C. R. Doering, K. V. Sargsyan, and L. M. Sander, *Multiscale Modeling & Simulation* **3**, 283 (2005).
- [25] O. Ovaskainen and B. Meerson, *Trends in ecology & evolution* **25**, 643 (2010).
- [26] I. Meyer and N. M. Shnerb, *Scientific Reports* **8**, 9726 (2018).
- [27] V. Elgart and A. Kamenev, *Physical Review E* **70**, 041106 (2004).
- [28] M. Assaf and B. Meerson, *Physical review letters* **97**, 200602 (2006).
- [29] R. Lande, *The American Naturalist* **142**, 911 (1993).
- [30] H. R. Akçakaya and P. Sjögren-Gulve, *Ecological Bulletins* pp. 9–21 (2000).
- [31] J. L. Sabo, E. E. Holmes, and P. Kareiva, *Ecology* **85**, 328 (2004).
- [32] S. P. Ellner, J. Fieberg, D. Ludwig, and C. Wilcox, *Conservation Biology* **16**, 258 (2002).
- [33] D. Matthies, I. Bräuer, W. Maibom, and T. Tschardtke, *Oikos* **105**, 481 (2004).
- [34] H. L. Jones and J. M. Diamond, *The Condor* **78**, 526 (1976).
- [35] G. Ferraz, G. J. Russell, P. C. Stouffer, R. O. Bierregaard, S. L. Pimm, and T. E. Lovejoy, *Proceedings of the National Academy of Sciences* **100**, 14069 (2003).
- [36] T. H. Keitt and H. E. Stanley, *Nature* **393**, 257 (1998).
- [37] E. Bertuzzo, S. Suweis, L. Mari, A. Maritan, I. Rodríguez-Iturbe, and A. Rinaldo, *Proceedings of the National Academy of Sciences* **108**, 4346 (2011).

- [38] I. Hanski, *Nature* **396**, 41 (1998).
- [39] H. Hinrichsen, *Advances in physics* **49**, 815 (2000).
- [40] H. Barghathi, S. Tackkett, and T. Vojta, *The European Physical Journal B* **90**, 129 (2017).
- [41] A. Liebhold, W. D. Koenig, and O. N. Bjørnstad, *Annu. Rev. Ecol. Evol. Syst.* **35**, 467 (2004).
- [42] S. P. Ellner, R. E. Snyder, P. B. Adler, and G. Hooker, *Ecology letters* (2018).
- [43] G. Barabás, R. D'Andrea, and S. M. Stump, *Ecological Monographs* **88**, 277 (2018).
- [44] S. J. Schreiber, *Journal of Difference Equations and Applications* **18**, 1381 (2012).
- [45] L. Ridolfi, P. D'Odorico, and F. Laio, *Noise-induced phenomena in the environmental sciences* (Cambridge University Press, 2011).